Convergent energy state-dependent antagonistic signalling by CART and NPY modulates the plasticity of forebrain neurons to regulate feeding in zebrafish

Devika S. Bodas[1,†], Aditi Maduskar[1,†], Tarun Kaniganti[1], Debia Wakhloo[1], Akilandeswari Balasubramanian[1], Nishikant Subhedar[1] and Aurnab Ghose[1,*]

Running title: CART-NPY antagonism in feeding circuit plasticity

[1] Indian Institute of Science Education and Research (IISER) Pune, Dr Homi Bhabha Road, Pune 411008, INDIA

[†] These authors contributed equally to this work

[*] Correspondence: Dr. Aurnab Ghose, Indian Institute of Science Education and Research (IISER) Pune, Dr Homi Bhaba Road, Pune 411008, INDIA.

Email: aurnab@iiserpune.ac.in

ABSTRACT

Dynamic re-configuration of circuit function subserves the flexibility of innate behaviours tuned to physiological states. Internal energy stores adaptively regulate feeding-associated behaviours by integrating opposing hunger and satiety signals at the level of neural circuits. Across vertebrate lineages, the neuropeptides CART and NPY have potent anorexic and orexic functions, respectively, and show energy state-dependent expression in interoceptive neurons. However, how the antagonistic activities of these peptides modulate circuit plasticity remains unclear.

Using behavioural, neuroanatomical and activity analysis in adult zebrafish, along with pharmacological interventions, we show that CART and NPY activities converge on a population of neurons in the dorsomedial telencephalon (Dm). While CART facilitates glutamatergic neurotransmission at the Dm, NPY dampens the response to glutamate. In energy-rich states, CART enhances NMDA receptor (NMDAR) function by PKA/PKC mediated phosphorylation of the NR1 subunit of the NMDAR complex. Conversely, starvation triggers NPY-mediated reduction in phosphorylated NR1 via calcineurin activation and inhibition of cAMP production leading to reduced responsiveness to glutamate.

Our data identify convergent integration of CART and NPY inputs by the Dm neurons to generate nutritional state-dependent circuit plasticity that is correlated with the behavioural switch induced by the opposing actions of satiety and hunger signals.

Keywords: Neuropeptide signalling; CART; NPY; feeding behaviour; behavioural flexibility; circuit plasticity, NMDA-R

INTRODUCTION

Adaptive regulation of feeding in response to internal energy needs is critical for survival. Internal sensory systems, located in the periphery and in the central nervous system, monitor energy homeostasis and signal satiety or hunger to the feeding-associated neural circuits. Hunger stimulates feeding circuits to generate motivational states that prioritise feeding and related activities over other behaviours. Conversely, satiety signals suppress the 'feeding drive' facilitating the pursuit of non-feeding-related behaviours. The flexibility of the feeding behaviour – exploiting or abandoning food resources – requires dynamic re-configuring of the activity states of the underlying circuits and the de-regulation of these processes forms the basis of eating disorders.

Neuropeptides, acting as hormones or local diffusive modulators convey nutritional state information to the nervous system (van den Pol, 2012). Neuropeptide-based neuromodulation of circuit function, via changes in neuron intrinsic properties or synaptic efficacy, may allow the same circuit to produce multiple outputs and behavioural outcomes (Nadim and Bucher, 2014). Neuropeptides typically engage G-protein coupled receptors (GPCRs) which, via intracellular signalling, may change circuit properties and extend acute signals of internal needs into long-lasting state changes mediated by biochemical hysteresis. For example, in the rodent arcuate nucleus (Arc), orexigenic neuropeptide ghrelin initiates an AMPK-mediated positive-feedback to potentiate glutamate release for extended periods (Yang et al., 2011). Consequently, several studies have implicated neuropeptides in mediating transitions between distinct behavioural states (Root et al., 2011; Elbaz et al., 2012; Flavell et al., 2013; Betley and Sternson, 2015).

Cocaine- and amphetamine-regulated transcript (CART) and Neuropeptide Y (NPY) are abundantly expressed neuropeptides conserved across vertebrate lineages. Both the neuropeptides have been implicated in a diverse range of physiological functions, including energy homoeostasis and food intake (Lau and Herzog, 2014; Subhedar et al., 2014; Singh et al., 2021)

CART is a potent anorexigenic agent and considered to be an endogenous satiety factor (Kristensen et al., 1998), especially in the framework of the Arc in the hypothalamus (Singh et al., 2021). Expression of CART increases in response to feeding in the Arc (Kristensen et al., 1998) and recent chemogenetic studies underscore the requirement of CART peptide in Arc neurons to inhibit food intake (Farzi et al., 2018). In contrast, hypothalamic NPY is orexigenic, and promotes food intake and energy conservation (Zhang et al., 2019). Starvation increases NPY expression in the Arc (Sainsbury and Zhang, 2010) and NPY-signalling from AgRP-expressing Arc neurons is critical for the sustained maintenance of the feeding drive (Chen et al., 2016).

Within the Arc, the coordinated co-regulation of the AgRP/NPY and the POMC/CART containing neurons in response to signals indicating metabolic states is well documented (Dietrich and Horvath, 2013; Andermann and Lowell, 2017). The physiologically opposing activities of these two populations and their effect on “second -order” neurons that drive satiety is a major regulator of the feeding behaviour (Garfield et al., 2015; Andermann and Lowell, 2017). However, the intracellular signalling engaged by these neuropeptides in the “second-order” neurons to re-configure the circuit properties and drive homoeostatic plasticity remains inadequately defined.

In zebrafish, NPY and CART are expressed in several brain areas, including the periventricular hypothalamus (homologous to mammalian Arc; Forlano and Cone, 2007) and the entopenduncular nucleus (EN) (Mathieu et al., 2002; Mukherjee et al., 2012; Yokobori et al., 2012; Akash et al., 2014). Starvation decreases CART mRNA expression in the periventricular hypothalamus and the EN (Nishio et al., 2012; Akash et al., 2014) while increasing NPY expression (Yokobori et al., 2012). Treatment with glucose also increases CART protein expression in the EN (Mukherjee et al., 2012). The zebrafish periventricular hypothalamus and the EN appear to be nutritional state sensitive interoceptive areas regulating energy homeostasis, in part via CART/NPY. Accordingly, treatment with NPY increases feeding in zebrafish and its action is mediated by the NPY Y1 receptor (Yokobori et al., 2012).

Despite the prominent involvement of CART and NPY in vertebrate energy homeostasis, it remains unclear how their activities re-configure the downstream, “second-order” circuits to meet behavioural demands. In this study, using zebrafish, we show that CART and NPY shape the feeding drive to match the prevailing energy states. The opposing energy state information represented by the two neuropeptides are integrated by a group of forebrain neurons by transforming the antagonistic signalling into dynamic changes in glutamatergic neurotransmission.

111 **MATERIALS AND METHODS**

112 **Animals**

113 Adult, wild-type zebrafish (*Danio rerio*) of both sexes were housed in stand-alone
114 housing systems and maintained on 14hL/10hD cycle. Fish were fed Ziegler feed
115 and live artemia 3 times a day. For calcium activity imaging experiments, adult
116 Tg(NeuroD:GcAMP6f) in the *nacre* background were used. All behavioural assays
117 and activity imaging experiments were performed between 10 am and 5 pm. No
118 randomization methods were used to allocate animals to different experimental
119 groups. The Institutional Animal Ethics Committee approved all the procedures
120 employed in this study. This study was not pre-registered.

121 **Chemicals**

122 The following reagents were administered to the zebrafish brain via
123 intracerebroventricular (icv) delivery. The concentrations indicated reflect the amount
124 delivered by the icv route. Rat CART peptide (55-102) (2 pmol in 1x PBS, Phoenix,
125 Cat. No. 003-62), full length human NPY peptide (10 pmol in 1x PBS, Sigma-Aldrich,
126 Cat. No. N5017), anti-CART antibody (1:500; gift from Drs. Lars Thim and Jes
127 Clausen, Novo Nordisk, Denmark); D -(+)- glucose monohydrate (40 nmol in 1x PBS,
128 glucose; Sigma-Aldrich, Cat. No. 49161), BIBP-3226 (100 pmol in 0.1% DMSO,
129 Sigma-Aldrich, Cat. No. B174), MK801 (0.015 nmol in 1x PBS, Sigma-Aldrich, Cat.
130 No. 77086), AP5 (0.1 nmol in 1x PBS, Tocris, Cat. No. 0106), KT5720 (1.4 pmol in
131 1x PBS, PKAi; Sigma-Aldrich, Cat. No. K3761), GF109206X (1.5 pmol in 1x PBS,
132 PKCi; Tocris, Cat. No. 0741), FK506 (0.13 nmol in 1x PBS, Sigma-Aldrich, Cat. No.
133 F4679), Forskolin (1.2 nmol in 0.1 % ethanol, Sigma-Aldrich, Cat. No. F6886). The
134 following reagents were used for procedures not requiring icv administration. 2-

135 Phenoxy Ethanol (1:2000 in system water, Sigma-Aldrich, Cat. No. P1126), D -(+)-
136 glucose monohydrate (Sigma-Aldrich, Cat. No. 49161), sucrose (Sigma-Aldrich, Cat.
137 No. S9703), paraformaldehyde (Sigma-Aldrich, Cat. No. 158127), poly-L- lysine
138 (Sigma-Aldrich, Cat. No. P8920), normal goat serum (Sigma-Aldrich, Cat. No. 9023),
139 bovine serum albumin (BSA) (SRL Pvt. Ltd., Cat. No. 83803), 1, 1', dioctadecyl-
140 3,3,3', 3'- tetramethylindo-carbocyanineperchlorate (DiI; Invitrogen Cat. No. D3911).

141 **Intracerebroventricular (icv) injections**

142 Fish were anaesthetised in 2-phenoxy ethanol (1:2000). The anaesthetised fish were
143 placed on a cotton bed containing anaesthesia solution to submerge its head. Icv
144 delivery protocol was modified after Yokogawa et al., 2007. Briefly, pharmacological
145 agent or vehicle was delivered directly into the ventricular space using an 31G
146 needle (Becton Dickinson Insulin Syringe U40 - 31G) attached via a catheter to a 10
147 µl Hamilton microsyringe. After injection, the fish were returned to their tanks and
148 allowed to recover before proceeding for either behavioural recordings or
149 immunohistochemistry. Unless otherwise indicated, 30 mins following injection, the
150 animals were subjected to behavioural task or sacrificed and the tissues processed
151 for immunofluorescence studies.

152 **Immunofluorescence**

153 Fish were subjected to icv injection with drug or vehicle and allowed to recover for 30
154 mins. After recovery, fish were anesthetised and craniotomised to expose the dorsal
155 surface of the brain. Samples were fixed in 4% PFA overnight at 4 ^{o}C. After fixation
156 for 12-14hrs (10 hrs for pNR1 staining), brain was dissected and cryoprotected with
157 25% sucrose prior to sectioning. Serial 15-20 µm thick sections of the entire
158 telencephalon were mounted onto lysine coated slides and stored at -40 ^{o}C till

159 further processing. Sections were allowed to dry for 2 hrs and washed with 0.5%
160 Triton X-100 in 1x PBS (PBST) three times for 10 min each). PBS of the following
161 composition was used: NaCl, 137 mM; KCL, 2.7 mM; Na_2HPO_4, 10 mM; KH_2PO_4 ,1.8
162 mM; pH-7.2. Sections were then blocked using 5% BSA in PBST for 1 hr prior to the
163 addition of primary antibodies and incubated overnight at 4°C. Next day, the washes
164 were repeated and sections blocked in 5% BSA/ 5% HIGS for 1 hr. The following
165 primary antibodies were used in this study: anti-p-ERK (1:700, Cell Signalling
166 technologies, Cat. No. 9101), anti- p-ERK (1:500, Abcam, Cat. No. ab50011), anti-
167 pNR1(Ser-897) (1:70, Millipore, Cat. No. ABN99), anti-Synaptophysin (1:100,
168 Invitrogen, Cat. No. PA1-1043).

169 Secondary antibodies were added and incubated at room temperature (RT) for 2.5
170 hrs in dark. The following secondary antibodies were used: Anti-rabbit Alexa Flour
171 488/568 (1:500, Invitrogen, Cat. No. A-11034/ A-11036) and anti-mouse Alexa Flour
172 488/568 (1:500, Invitrogen, Cat. No. A-11029/A-11031). Sections were washed and
173 mounted in media (0.5% N propyl gallate, 70% glycerol ,1M tris pH8.0) containing
174 4′,6-diamidino-2-phenylindole (DAPI) (Invitrogen, Cat. No. D1306). Sections were
175 observed under Axioimager Z1 (Zeiss) epifluorescence microscope and
176 representative images were acquired using confocal microscope (SP8, Leica or LSM
177 780, Zeiss). In order to ensure reliable comparisons across different groups and
178 maintain stringency in tissue preparation and staining conditions, all the brain
179 sections were processed concurrently under identical conditions.

180 **Feeding Behaviour**

181 Fish were isolated from home tanks and housed singly in the experimental tank prior
182 to behavioural analysis. Fig. S1 outlines the protocol followed for all feeding
183 behaviour experiments. Briefly, for first two days of habituation, the experimental

184 tanks were moved to the recording chamber and the fish were fed floating, insoluble
185 food pellets (15 ± 5 pellets; Taiyo) for 1 hour before returning to the housing rack.
186 For habituation to injection and handling stress, the fish were anesthetised and
187 delivered mock icv injection (saline, 0.9% NaCl) on day 4 and day 5. Fish were
188 allowed to recover in recording chamber for 1 hour, before returning the tanks to the
189 housing racks. Depending on the experiment, the fish were either starved or given
190 pellet food for 1 hr on these days. Fish were observed on all days of the protocol for
191 any anxious/abnormal behaviour. Fish exhibiting such behaviours were not included
192 for further analysis. On the day of the experiment, fish were anaesthetized and icv
193 injected with appropriate reagents or vehicle. Following a recovery period of 15 mins,
194 floating pellets of food (~15 ± 5) were added to the tank and the behaviour of the fish
195 recorded individually using a video recorder (Sony Handycam DCR SR-47 and DCR
196 SR-20) for an hour. All recordings were conducted under conditions of uniform
197 lighting and temperature. In all experiments, animals deprived of food for 2.5 days
198 are referred to as 'starved' and those that received food as per regular feeding
199 schedule, and used for experiments within one hour of feeding, are referred to as
200 'fed'. The recorded videos were not blinded and the number of biting attempts was
201 counted manually. The data was plotted as the cumulative number of biting attempts
202 displayed during 60 mins.

203 **Calcium imaging**

204 Starved, adult Tg(NeuroD:GcAMP6f) fish were injected with either vehicle or drugs.
205 After 15 min, the fish were anesthetized in ice cold HEPES-based Ringer's solution
206 [NaCl, 134 mM; $MgCl_2$, 1.2 mM; $CaCl_2$, 2.1 mM; KCl, 2.9 mM; HEPES, 10 mM;
207 Sucrose, 10 mM (for glucose-deprivation) or Glucose, 10 mM (to mimic satiety); pH
208 7.2] bubbled with 100% O_2 and craniotomised to dissect the telencephalon. The

209 optic nerves were cut off and the telencephalon was dissected out by cutting just
210 rostral to habenula. The telencephalon was carefully lifted from the base while
211 removing the ventral connections and immediately transferred to Ringer's solution
212 supplemented with 100% O_2.

213 For *ex vivo* whole-brain preparations, starved fish were anesthetised in ice-cold
214 HEPES-based Ringer's solution. First the optic nerves and connections on the
215 ventral side were severed and the whole brain was dissected out by separating it
216 from spinal cord.

217 The intact telencephalon or the whole brain was mounted in 4% low-melt agarose (in
218 50% Ringer's) on to a RC-26 GLP chamber from Warner Instruments (Cat. No.
219 640236). The imaging chamber was mounted onto an upright confocal microscope
220 (Leica TCS SP8 MP) and continuously perfused with HEPES-based Ringer's
221 solution via am VC 8 perfusion system (Warner Instruments, Cat. No.640186)
222 directly triggered by the recording software (Leica). Images were acquired at 9.8 Hz
223 at a resolution of 512 x 300 pixels using a 488 nm laser in the resonant, bi-directional
224 scanning mode and a 25x water-immersion objective (N.A 0.95). Baseline imaging
225 was performed for 1 min before the start of the glutamate stimulation. Glutamate (75
226 μM, in Ringer's buffer) was perfused from the 2nd to 5th mins and subsequently
227 washed out.

228 **Data Analysis**

229 Immunofluorescence: The tissue slices were observed under Axioimager Z1 (Zeiss,
230 20x objective 0.8 NA) with the imaging conditions kept constant across all treatment
231 groups. The number of p-ERK positive cells in Dm were scored manually. To avoid

232 over estimation of cell count due to sectioning, the cell numbers were corrected
233 using Abercrombie's method (Abercrombie, 1946).

234 Average pNR1 intensity per cell in Dm was calculated using IMAGE J. The exposure
235 time and other imaging conditions were kept constant for every sample processed.
236 Each neuron in Dm was selected using manual thresholding on the DAPI filter, and
237 the mean intensity of pNR1 per neuron was calculated using IMAGEJ in-built
238 algorithms. Images were acquired using a 40x objective (1.3 NA) on a SP8 confocal
239 microscope (Leica).

240 Calcium imaging: Measurements of population level calcium activity in Dm were
241 performed using ImageJ and the average GCaMP6f fluorescence in the Dm at each
242 time point was calculated. For this, we manually marked an ROI encompassing the
243 Dm using the wand tool in ImageJ on maximum intensity projection of all the frames.
244 This ROI was then applied to the time lapse series and the baseline fluorescence
245 (F0) estimated by taking the average of fluorescence values of 620 frames before
246 the start of glutamate treatment. The relative change in fluorescence ($\Delta F/F0$), was
247 calculated using the formula F-F0/F0, where F stands for the fluorescence value at a
248 given time. The maximum response amplitude, i.e., maximum $\Delta F/F0$ was determined
249 from the temporal sequence using Microsoft Excel. The total magnitude of the
250 response was calculated by computing the area-under-the-curve (AUC), from start of
251 glutamate treatment to end of the washout period, in the GraphPad Prism ver 8
252 software.

253 Feeding assay: Videos were analysed manually at 1.5x speed and the number of
254 biting attempts were scored. The data were distributed in bins of 15 mins and
255 cumulative biting attempts were plotted using GraphPad Prism ver 8 software.

256 **Statistical Analysis**

257 Data were tested for normality using the Shapiro-Wilk test in GraphPad Prism 8.
258 Behaviour and immunohistochemical data were subjected to the t-test with Welch's
259 correction or the Mann-Whitney test (for single comparison) and One-Way ANOVA
260 with the Tukey's test or Two-way ANOVA, with Bonferroni's post-hoc analysis (for
261 multiple comparisons). All values are expressed as mean ± SEM of the group in the
262 Results section and differences were considered significant at $p<0.05$. Graphs were
263 plotted using the GraphPad Prism 8.0 software. Data for feeding drive are
264 represented as columns (with error bars marking mean± SEM) of cumulative biting
265 attempts in 15 min bins over a 1-hour period. Change in GCaMP6f fluorescence over
266 time is represented as XY plots with the dark line representing mean and the dotted
267 lines denote the SEM. All data shown as violin plots have the thicker dashed line
268 representing median and dotted lines representing first and third quartile.

269

RESULTS

CART neuropeptide mediates satiety during energy-rich metabolic states

To quantitatively evaluate the feeding drive of adult zebrafish, we developed a behavioural assay that scores the number of biting attempts made by the animal upon presentation of solid, floating food pellets (see Methods and Fig. S1). We found that hungry fish made many more biting attempts over a period of 1 h (794±57.46; Fig. 1 A) compared to fed animals (338.8±70.4; Fig. 1 A). Analysis of the number of biting attempts across 15 min bins revealed cumulated difference over the 1 h period. To rule out contributions from altered locomotion or stress-induced behaviours, we evaluated animals under fed and starved conditions for locomotion kinematics and indicators of anxiety-associated behaviours but found no change in these parameters (Fig. S2).

To directly assess the role of CART neuropeptide in anorexia, we delivered CART peptide (55-102 aa) via the intracerebroventricular (icv) route to the brain of starved fish. Strikingly, exogenous administration of CART directly to the brain was sufficient to induce acute anorexia in starved fish (36.21±14.89; Fig. 1 B) compared to starved animals injected with vehicle (829.4±58.03 Fig. 1 B). However, CART treatment did not induce anxiety-like behaviours or modify locomotion (Fig. S2).

To test if central application of glucose resulted in anorexia, glucose was directly introduced via the icv route to the brains of starved fish to mimic energy surfeit conditions and preclude peripheral inputs. In contrast to starved animals (852±133.3), glucose-injected fish displayed a dramatic reduction in biting attempts (221.2±33.67; Fig. 1 C). As CART promotes anorexia (Lau and Herzog, 2014b) and CART peptide expression is sensitive to metabolic states in the zebrafish brains

294 (Mukherjee et al., 2012; Akash et al., 2014), we used an immunoneutralising
295 antibody against the CART peptide to test if endogenous CART signalling mediates
296 the glucose-induced reduction in feeding. Indeed, glucose-induced anorexia in
297 starved animals was alleviated in the presence of CART immunoneutralising
298 antibodies also introduced by the icv route (629.9±79.31; Fig 1 C). CART antibodies
299 on their own did not influence the feeding behaviour (658.4±67.13; Fig 1 C).

300 Collectively, these results establish the role of CART neuropeptide signalling in the
301 zebrafish brain in mediating the reduction in food intake behaviour during energy-rich
302 metabolic states.

303

304 **CART signalling alters the activity of telencephalic Dm neurons**

305 The entopeduncular nucleus (EN) in the ventral telencephalon as well as
306 periventricular hypothalamic nuclei, like the nucleus lateralis tuberis (NLT), show
307 energy-state dependent changes in CART mRNA expression (Akash et al., 2014).
308 Administration of glucose also increased the number of CART peptide expressing
309 cells in the EN and the NLT (Fig. S3; Mukherjee et al., 2012).

310 CART immunofluorescence analysis of transverse sections of the zebrafish
311 telencephalon was used to evaluate the projections from the EN. CART-positive EN
312 soma was found to project to the dorsomedial telencephalon (Dm; Fig S4 A). This is
313 consistent with earlier reports indicating that EN neurons project to the Dm (Turner et
314 al., 2016). We used the lipophilic dye, DiI, to confirm if the Dm receives projections
315 from EN and other energy status-responsive interoceptive areas. DiI-positive fibres
316 from the Dm typically extended caudally and ventrally and merged with the lateral
317 forebrain bundle. Labelled cells were found in the ipsilateral EN (Fig S4 B,C). Fibres

318 were also traced caudally into the hypothalamus and labelled somata were located in
319 the preglomerular nucleus and the NLT (Fig S4 B,D). This connectivity is consistent
320 with previous reports from teleost fish, including zebrafish (Yáñez et al., 2017). Dual
321 immunostaining for CART peptide and the presynaptic marker synaptophysin
322 revealed significant co-localisation, indicating the presence of CART in presynaptic
323 terminals at the Dm (Fig S4 F). However, no CART expressing somata were
324 detected in the Dm.

325 Collectively, these results demonstrate that CART peptide expression in EN and the
326 periventricular hypothalamus is controlled by metabolic states and these areas send
327 projections to the Dm (Fig. S4 E). This connectivity suggested that Dm neurons
328 could be responsive to energy state-dependent CART activity. To assess the
329 involvement of Dm, we used phosphorylated ERK (p-ERK), a marker of recent
330 neuronal activity (Randlett et al., 2015).

331 Starved fish injected with CART peptide via the icv route had an elevated number of
332 p-ERK positive neurons in the Dm (533.9±89.04) in comparison to starved, vehicle-
333 injected animals (159.5±34.52) (Fig 2 A-C). As these data suggest a CART-mediated
334 increase in neuronal activity in the Dm, we tested if feeding was sufficient to induce
335 neuronal activation of the Dm neurons by comparing starved and recently fed fish
336 (where endogenous levels of CART are high; Fig S3). Remarkably, Dm also shows
337 increased neuronal activity (423.2±26.61) in fed fish as compared to starved controls
338 (180.0±12.42) (Fig 2 D-F). The subpopulation of Dm neurons responding to
339 CART/fed states was limited to a ~ 250 μm region rostral to the level of the anterior
340 commissure (Fig 2 G-I).

341 These findings suggest that enhancement of CART function at the Dm, possibly by
342 the energy state responsive neurons of the EN and the periventricular hypothalamus,

343 results in increased neuronal activity. However, the possibility of additional inputs
344 from other CART-ergic sources cannot be ruled out

345

346 **CART modulates NMDAR signalling to regulate the feeding behaviour and the**
347 **activity of Dm neurons**

348 The dorsal telencephalon of teleosts, including the Dm, is rich in glutamatergic
349 neurons (Aoki et al., 2013) and shows significant binding of labelled kainate and l-
350 glutamate (Tong et al., 1992) implicating glutamatergic neurotransmission. Studies in
351 rodents have previously implicated NMDA receptor (NMDAR)-mediated CART
352 signalling in the context of innate fear processing (Rale et al., 2017) and nociceptive
353 transmission (Chiu et al., 2010) in rat. We investigated NMDAR signalling in CART-
354 mediated regulation of feeding behaviour using NMDAR antagonists. Icv delivery of
355 AP5 (competitive NMDAR antagonist) alone in starved fish showed no difference in
356 biting attempts (845.3±89.82; Fig 3 A) as compared to vehicle controls (812.8±84.38.
357 However, CART-induced anorexia (47.33±11.4) was abrogated when CART peptide
358 and AP5 were co-administered (488.7±42.03; Fig 3 A). Application of the non-
359 competitive NMDAR antagonist, MK801 produced similar results (Fig S5 A).

360 AP5 was co-injected with CART peptide in starved animals to evaluate the role of
361 NMDAR signalling in modulating the activity of the Dm neurons. Neuronal activity in
362 the Dm, indicated by the number of p-ERK positive neurons, was robustly attenuated
363 in CART peptide and AP5-treated fish (165.7±11.87) compared to animals injected
364 with only CART peptide (312±18.2; Fig 3 B). AP5 alone (125.2±6.96) did not
365 influence the number of p-ERK positive Dm neurons as compared to those in vehicle

366 controls (126.7±13.35; Fig 3 B). The application of MK801 produced similar results
367 (Fig S5 B).

368 Together these data indicate that NMDAR activity is required for processing CART-
369 induced satiety signals in the Dm neurons.

370

371 **PKC and PKA phosphorylate NR1 to mediate the modulation of NMDAR**
372 **signalling by CART**

373 Protein kinase C (PKC) and Protein kinase A (PKA) mediated phosphorylation of the
374 NR1 subunit of the mammalian NMDAR is known to potentiate NMDAR signalling by
375 increasing the channel opening probability and enhancing calcium permeability (Lan
376 et al., 2001; Skeberdis et al., 2006). PKA and PKC have also been implicated in
377 CART-signalling in *in vitro* experiments (Chiu et al., 2010). We next evaluated PKA
378 and PKC function in CART signalling using specific pharmacological inhibitors of
379 PKA and PKC kinase activity.

380 KT5720 (selective PKA inhibitor, PKAi), when co-injected into the ventricle of starved
381 fish along with CART peptide, alleviated (697.49±105.59) the strong reduction in the
382 number of biting attempts induced by CART peptide alone (30.33±10.61 Fig. 4 A).
383 The inhibitor on its own had no significant effect on the feeding drive
384 (713.92±215.68) as compared to starved control animals (782.9± 71.70; Fig. 4 A).

385 Parallel studies evaluating the activity of Dm neurons revealed a robust suppression
386 of CART-induced neuronal activation in fish co-administered with PKAi and CART
387 peptide (158.1±56.47; Fig. 4 B) compared to those injected with only CART peptide
388 (554.5±82.75; Fig. 4 B).

389 As observed for PKAi, inhibition of PKC by GF109206X (selective PKC inhibitor,
390 PKCi) also reversed the suppression of the feeding drive by CART peptide (489.8±
391 29.38 for PKCi + CART and 29.83±6.76 for CART alone; Fig. 4 C) and abrogated the
392 activation of Dm neurons by CART (247.7±28.99 for PKCi + CART and 464.9± 19.57
393 for CART alone; Fig. 4 D).

394 Together, these data implicate PKA and PKC activity in CART-mediated activation of
395 Dm neurons and satiety. PKC and PKA are known to phosphorylate mouse NR1 at
396 multiple residues, including serine 897 (Chen and Roche, 2007). Specific antibodies
397 against phosphoserine 897 of the mouse NR1 (pNR1) were used to evaluate the
398 status of NR1 phosphorylation in the Dm neurons. While the Dm of CART-treated
399 animals displayed strong pNR1 fluorescence (892.1±5), co-injection of PKAi, PKCi,
400 and CART peptide greatly reduced the pNR1 signal (505.9±2.02) (Fig. 4 E-G).

401 Collectively, these data identify CART signalling mediated phosphorylation of NR1
402 via PKA and PKC. The heightened neuronal activity of Dm neurons could be
403 attributed to the potentiation of NMDAR function driven by NR1 phosphorylation.

404

405 **CART treatment enhances NMDA receptor function resulting in increased**
406 **sensitivity of Dm neurons to excitatory stimuli**

407 Phosphorylation of NR1 subunit of NMDARs by PKA and PKC is known to enhance
408 NMDAR signalling (Lan et al., 2001; Skeberdis et al., 2006). We speculated that a
409 CART-induced increase in phosphorylation of NMDARs would sensitise and
410 enhance the response of Dm neurons to glutamatergic inputs. We tested this
411 hypothesis directly using the Tg(NeuroD:GCaMP6f) zebrafish, which shows strong
412 expression of the genetically-encoded calcium sensor, GCaMP6f in the Dm. *Ex vivo*

413 preparations of the intact telencephalon were dissected from starved animals treated
414 earlier with either saline or CART via the icv route (see Methods and Fig. 5 A). Dm
415 neurons of vehicle-treated animals failed to respond to glutamate stimulation.
416 However, CART peptide-treated animals showed heightened activity of Dm neurons
417 in response to glutamate. Both the maximum amplitude of the response (0.44±0.09
418 for vehicle control and 3.43±0.6 for CART) and the magnitude (area under the curve)
419 of the response (69.04±15.29 for vehicle control and 522.6±94.66 for CART) was
420 substantially higher in starved animals receiving CART peptide (Fig. 5 B-E). Co-
421 treatment of AP5 along with CART peptide prevented the activation of the Dm
422 neurons by glutamate (maximum amplitude:0.29±0.11 compared to 1.724±0.44 for
423 CART alone; magnitude: 64.76±10.88 compared to 230.7± 41.33 for CART alone)
424 and underscored the involvement of NMDAR signalling (Fig. 5 F-H).

425 To determine if the change in the glutamate sensitivity of Dm neurons in response to
426 CART required PKA and PKC activity, we co-administered selective PKA and PKC
427 inhibitors along with CART. Interestingly, blocking PKA and PKC activity abolished
428 the CART-induced increased sensitivity of Dm neurons to glutamate (Fig.5 I-K). The
429 maximum amplitude of the response was reduced to 0.21±0.06 (PKAi+PKCi+CART)
430 from 2.48±0.43 (CART alone), and the magnitude of the response dropped from
431 380.3±75.86 (CART alone) to 33.39±7.71 (PKAi+PKCi+CART).

432 Together these data suggest that CART signalling via PKA and PKC sensitizes
433 NMDA receptors in the Dm neurons, possibly via post-translational modification of
434 NR1 subunits, leading to the enhanced activation of these neurons. This CART
435 neuropeptide-mediated response of the Dm neurons may constitute a neural
436 representation of the sated state of the animal.

437

438 **The activity of Dm neurons is tuned to changes in energy states**

439 To assess if Dm exhibits heightened activity in energy-rich metabolic states, we used
440 *ex vivo* whole-brain preparations from starved animals maintained in sucrose (to
441 maintain gluco-deprived conditions). Following initial evaluation of the response of
442 Dm neurons to glutamate stimulation, the preparation was incubated in glucose to
443 mimic energy-rich conditions and re-evaluated for neural activity in response to
444 glutamate stimulation (see Methods and Fig. 6 A).

445 Glutamate stimulation of whole-brains of starved animals maintained in gluco-
446 deprived conditions (pre-glucose) failed to activate Dm neurons (maximum amplitude
447 of response: 0.243±0.1 and magnitude of response: 48.29±14.71; Fig 6 B-D).
448 However, upon incubation of the same whole-brain preparation with 10 mM glucose
449 for 30 mins (post-glucose), the Dm neurons responded strongly to glutamate
450 stimulation (maximum amplitude of response: 2.33±0.29 and magnitude of response:
451 485±48.05; Fig 6 B-D). In control experiments, whole-brain preparations from
452 starved animals were maintained throughout in glucose-free media, including the 30
453 min period between the two glutamate stimulations. In these control experiments,
454 Dm neurons did not respond to glutamatergic stimulation either before (pre-control)
455 or after the 30 min control incubation (post-control; Fig 6 B-D).

456 These experiments indicate that activity in the Dm is tuned to changes in glucose
457 levels in the brain and neuronal activity in Dm is correlated to energy states. As
458 CART levels are sensitive to metabolic states (Fig S3; Mukherjee et al., 2012; Akash
459 et al., 2014), the glucosensitive neurons of the EN and hypothalamus may contribute
460 to elevating endogenous CART signalling at the Dm neurons to mediate this effect.
461 Interestingly, the change in Dm activity appears to be independent of peripheral
462 mediators of energy homeostasis.

463

464 **NPY promotes food intake in zebrafish**

465 Beyond sensing energy sufficiency, interoceptive awareness is also expected to
466 involve signals indicating depletion of energy stores. Neuropeptide Y (NPY) is a
467 potent orexigenic neuropeptide (Zhang et al., 2019), which is expressed in the EN
468 and periventricular hypothalamic regions of teleosts, including zebrafish (Mathieu et
469 al., 2002; Mukherjee et al., 2012; Akash et al., 2014; Turner et al., 2016) and
470 regulates the feeding behaviour (Yokobori et al., 2012). We tested if NPY signalling
471 regulated zebrafish feeding drive in a manner obverse to that of CART.

472 A selective NPY receptor Y1R (Y1R) antagonist, BIBP-3226 (BIBP; Doods et al.,
473 1995; Yokobori et al., 2012; Kaniganti et al., 2021), was administered to starved fish
474 to evaluate endogenous NPY signalling in regulating the feeding drive. Compared to
475 vehicle-injected starved animals (789±69.46), BIBP introduced by the icv route
476 robustly suppressed the biting frequency (144.7±21.57; Fig. 7 A) and is consistent
477 with earlier reports (Yokobori et al., 2012).

478 To evaluate if NPY could increase the feeding drive, we intracerebroventricularly
479 introduced NPY peptide into recently fed fish. As expected, vehicle-injected fed fish
480 made infrequent biting attempts (338.8±70.4) while NPY injected animals showed
481 increased feeding drive (983.7±75.84) that was comparable with starved animals
482 (Fig. 7 B). However, there was no change in locomotion or anxiety-like behaviours in
483 NPY-treated animals (Fig. S2).

484

485 **NPY signalling converges on the Dm neurons to decrease neuronal activity**

486 Increased expression of NPY in response to starvation has been reported in several
487 species (Loh et al., 2015), as also observed in the hypothalamic nuclei of zebrafish
488 (Yokobori et al., 2012). Compared to fed zebrafish, the number of NPY positive
489 neurons increased in the EN and the hypothalamic nucleus recessus lateralis (NRL)
490 of starved animals (Fig. S6 A-F).

491 In transverse slices of the telencephalon, NPY-expressing EN soma was found to
492 project to the Dm (Fig S6 G) similar to what was seen for CART-positive EN
493 neurons. EN to Dm projections is consistent with previous reports (Turner et al.,
494 2016). Together with DiI tracing experiments reported earlier (Fig. S4 B-D), the
495 connectivity of periventricular hypothalamic nuclei and the EN to Dm (Fig. S6 H)
496 raises the possibility of NPY signalling also converging on the Dm and opposing
497 CART activity. We tested this possibility by evaluating the activity of the Dm neurons
498 in response to NPY.

499 Icv administration of NPY to recently fed animals reduced the number of p-ERK
500 positive Dm neurons (109.5±4.74) compared to vehicle controls (353.5±49.73; Fig. 7
501 C-E). Thus, the difference in the activity of Dm neurons observed between fed and
502 starved animals (Fig. 2 D-F) can be partially explained by the opposing orexic and
503 anorexic signalling by NPY and CART neuropeptides, respectively.

504 As CART signalling increased the phosphorylation of the NR1 subunit of NMDAR to
505 increase neuronal activity, we tested if the reduction of Dm activity following NPY-
506 treatment was a result of decreased NR1 phosphorylation. Indeed, glucose-
507 stimulated (satiety mimic) pNR1 fluorescence (944.3±2.98) was substantially
508 decreased (478.2±2.03) when NPY peptide was co-injected with glucose into the
509 brain of starved fish (Fig. 7 F-H).

510 These data identify NPY-signalling, originating from the energy state sensitive
511 populations of the hypothalamus and EN under energy poor metabolic states, in
512 modulating zebrafish feeding behaviour. NPY-signalling converges on the Dm
513 neurons, acts antagonistically to CART to reduce NR1 phosphorylation and
514 decreases neuronal activity at the Dm.

515

516 **NPY signalling reduced the glutamate responsiveness of Dm neurons**

517 To directly test if NPY signalling reduced the response of Dm neurons to
518 glutamatergic stimulation, we evaluated the Dm activity in the Tg(NeuroD:GCaMP6f)
519 zebrafish line. *Ex vivo* preparations of the intact telencephalon were dissected from
520 starved animals treated earlier with either glucose (satiety mimic) or glucose and
521 NPY via the icv route.

522 As expected, Dm of glucose injected animals responded to glutamate stimulation
523 (maximum amplitude of response: 0.39±0.09 and magnitude of response:
524 75.45±12.93). However, the response to glutamate was substantially damped in the
525 Dm of fish co-injected with glucose and NPY (maximum amplitude of response:
526 0.13±0.06 and magnitude of response: 28.43±4.7; Fig. 7 I-K).

527 These data show that NPY signalling alters the responsiveness of Dm neurons to
528 glutamate and this altered activity state of Dm may be a neuronal representation of
529 the energy deficit conditions. The orexic NPY signalling and the anorexic activities of
530 the CART neuropeptide converge on the Dm neurons. Dm thus appears to be an
531 important integrative centre whose activity is correlated with the homoeostatic
532 regulation of feeding.

533

534 **Orexic signalling by NPY is mediated by the activation of calcineurin and**
535 **inhibition of adenylyl cyclase**

536 Our data identify PKA and PKC mediated phosphorylation of NR1 in the Dm neurons
537 in response to CART in inducing satiety. Further, NPY signalling appears to oppose
538 CART function, including the dephosphorylation of NR1 (Fig 7 H). Thus, we
539 investigated NPY-induced signalling that could oppose CART function.

540 In mammals, NPY increases the activity of the protein phosphatase calcineurin
541 (Chen et al., 2005; Sajdyk et al., 2008) and calcineurin is known to dephosphorylate
542 NR1 (Choe et al., 2005). We blocked calcineurin activity using FK506 (calcineurin
543 inhibitor) in NPY peptide-treated fed fish and evaluated their feeding behaviour.
544 FK506 alone (222±57.39) did not show any significant effect on the number of biting
545 attempts as compared to vehicle controls (291.4±79.85; Fig 8 A). However, the co-
546 injection of FK506 along with NPY (368±50.97) reversed NPY induced orexia
547 (954.7±67.55; Fig 8 A).

548 To test if blocking calcineurin activity affects NPY induced reduction in Dm activity,
549 we co-injected FK506 and NPY peptide in fed fish. Treatment with the FK506 alone
550 (299.8±38.11) did not affect the number of p-ERK positive neurons in the Dm of fed
551 fish (409.6±32.62; Fig 8 B). However, blocking calcineurin activity in NPY treated fish
552 (502.4±56.7) abrogated NPY-induced (111±9.38) reduction in p-ERK positive
553 neurons in Dm.

554 We have demonstrated that NPY function in regulating food intake in zebrafish is via
555 the Y1 receptor (Fig. 7 A). NPY Y1R is G protein receptor that inhibits adenylyl
556 cyclase activity (Molosh et al., 2013). A fall in cAMP production by adenylyl cyclase
557 is expected to reduce the activation of PKA, and PKA is critical for CART signalling

558 (Fig 4 A,B). Therefore, we activated adenylyl cyclase with Forskolin (an adenylyl
559 cyclase agonist) in fed fish co-treated with NPY. Forskolin alone (236±77.40) did not
560 influence the number of biting attempts as compared to vehicle controls
561 (261.8±86.98; Fig. 8 C); however, application of Forskolin in NPY co-injected fed fish
562 reversed (194.7±40.7) NPY induced orexia (929±96.86; Fig. 8 C).

563 Forskolin co-administered along with NPY in fed fish, via the icv route, alleviated
564 (304.1±49.90) NPY-mediated reduction of p-ERK positive neurons in the Dm of fed
565 animals (145.1±23.68; Fig. 8 D). Treatment with forskolin alone (223.8±20.05) was
566 comparable to vehicle-injected fed fish (296.6±56.19; Fig 8 D).

567 Collectively, these experiments demonstrate that orexic NPY signalling is mediated
568 by the downregulation of cAMP activity and upregulation of calcineurin activity, which
569 decreases the activity of Dm neurons via reduced phosphorylation of NR1. NPY-
570 signalling is antagonistic to CART-induced phosphorylation of NR1 and the energy-
571 state dependent expression of CART/NPY results in the bimodal regulation of Dm
572 activity and feeding behaviour.

573

DISCUSSION

The flexibility of innate, motivated behaviours is driven by context-dependent recruitment and outputs of the underlying neural circuits (Sternson, 2013; Flavell et al., 2020). Neuromodulator-based signalling has emerged as a key mechanism facilitating reconfiguration of circuit activity (Lee and Dan, 2012). For instance, state changes between component behaviours in *C. elegans* foraging is regulated by the differential recruitment of circuits by the opposing activities of serotonin and the PDF neuropeptide (Flavell et al., 2013). Neuropeptide activities may also change the response of specific neurons or circuits. Peptidergic modulation of the worm ASH neuron mediates feeding state-dependent nociceptive responses (Ezcurra et al., 2016). Similarly, NPY-signalling regulates the sensitivity of zebrafish olfactory receptor neurons in response to hunger (Kaniganti et al., 2021).

Homoeostasis necessitates altering food intake in response to changing energy stores. Therefore, the neural circuits regulating food intake need to be dynamic and responsive to physiological states. Neuropeptidergic signalling may represent energy state information and facilitate biochemical modulation of synaptic transmission to regulate food intake-associated behaviours. Indeed, a diverse and complicated network of peptidergic activity, both peripheral and central, influence the plasticity of neural circuits regulating food intake (Crespo et al., 2014). However, the neuropeptide-induced signalling facilitating the integration of opposing energy state signals to generate appropriate behavioural outputs remains poorly understood.

In the mammalian Arc, the POMC/CART-expressing neurons of the Arc release α-MSH onto the MC4R-expressing neurons of the paraventricular hypothalamic nucleus (PVH) to enhance glutamatergic neurotransmission and induce satiety (Fenselau et al., 2017). Conversely, the GABAergic AgRP/NPY neurons on the other

599 hand provide an inhibitory tone onto MC4R-expressing PVH neurons to promote
600 food intake (Fenselau et al., 2017). While opposing inputs from the Arc converge
601 onto the PVH neurons, the intracellular mechanisms recruited by these peptidergic
602 neuromodulators are inadequately characterised.

603 We demonstrate the convergence of antagonistic intracellular signalling mediated by
604 the anorexic neuropeptide CART and the orexic NPY on a zebrafish telencephalic
605 neuronal population to reconfigure its activity. Energy state sensitive expression of
606 the neuropeptides impose opposing biochemical constraints on their target neurons
607 at the dorsal telencephalon via the modulation of NMDAR function and regulate the
608 feeding behaviour.

609 We show that not only do the endogenous activities of CART and NPY modulate the
610 feeding drive, but the intracerebroventricular delivery of these peptides acutely alters
611 food intake in the expected direction. We limit our analysis to intracerebroventricular
612 (icv) delivery of bioactive molecules and pharmacological agents to focus on central
613 activities and avoid potential confounds originating from peripheral inputs. Consistent
614 with earlier work (Subhedar et al., 2011; Mukherjee et al., 2012; Yokobori et al.,
615 2012; Akash et al., 2014), we also find that expression of CART peptide increases,
616 under energy-rich conditions, in energy state interoceptive regions of the
617 periventricular hypothalamus and the EN of zebrafish while NPY expression
618 increases upon starvation.

619 Anatomical analysis indicated that the peptidergic neurons of the periventricular
620 hypothalamus and the EN project to the Dorsomedial telencephalon (Dm) and
621 suggested that the latter population may be the target for CART or NPY, under
622 different metabolic states. The connectivity observed in our tracing studies is in line
623 with observations reported in other teleosts (Kanwal et al., 1988), including zebrafish

624 (Turner et al., 2016; Yáñez et al., 2017). Thus, our subsequent studies focussed on
625 the neuronal activity at the Dm, in response to CART and NPY.

626 Using p-ERK as a readout of recent neuronal activity and calcium imaging of a
627 genetically encoded calcium sensor, we found that energy-rich states resulting from
628 recent feeding (and consequent increase in endogenous CART neuropeptide) or
629 exogenous application of CART peptide to the brain led to heightened activity of the
630 Dm neurons. The increased activity of the Dm neurons was found to be NMDAR
631 dependent and blocking NMDAR signalling reduced Dm activity and CART-mediated
632 anorexia.

633 Studies in rodents have previously reported the involvement of NMDA receptors in
634 the regulation of food intake. Under satiety conditions, NMDA receptors in the
635 hindbrain are required for CCK induced reduction of food intake (Wright et al., 2011).
636 NMDAR function has also been implicated in leptin (Neyens et al., 2020) and
637 PACAP (Resch et al., 2014) mediated reduction in food intake. Furthermore,
638 NMDAR activity in the lateral hypothalamus regulates food intake in hungry animals
639 (Stanley et al., 2011), while it is necessary for the activity of the AgRP-expressing
640 neurons to establish the starvation state (Liu et al., 2012). In addition, CART function
641 in processing innate fear in the central amygdala (Rale et al., 2017) and nociception
642 by sensory neurons (Chiu et al., 2010) also involve NMDAR function and may
643 represent a common modality in CART signalling.

644 Further investigations identified PKA and PKC activities in mediating CART induced
645 anorexia since inhibiting the activity of either kinases led to the restoration of food
646 intake and decreased neuronal activation in the Dm. Using phosphospecific NR1
647 antibodies we found that CART induced activation of PKA and PKC results in
648 phosphorylation of NR1 on specific residues.

649 Phosphorylation of NR1 by PKC and PKA has been known to enhance NMDAR
650 signalling by increasing both the Ca^{2+} permeability (Skeberdis et al., 2006) and the
651 opening probability of the receptor complex (Lan et al., 2001). Thus CART-induced
652 phosphorylation is likely to increase the responsiveness of Dm neurons to
653 glutamatergic inputs and is consistent with our results showing heightened calcium
654 response of Dm neurons upon stimulation by glutamate.

655 The modulation of Dm activity by endogenous CART release in response to energy-
656 rich conditions was demonstrated using calcium imaging of *ex vivo* whole-brain
657 preparations where the inputs from the hypothalamus and EN are preserved. Brains
658 isolated from starved animals (low endogenous CART and high endogenous NPY)
659 failed to respond to glutamate when maintained under glucose deprived conditions.
660 However, incubation with glucose restored glutamate responsiveness and suggests
661 altered inputs (including CART) from the glucose-sensing interoceptive areas. While
662 this response may involve modulatory inputs to the Dm not limited to CART, it is
663 consistent with our observations of CART function. Importantly, as the experimental
664 preparation precludes peripheral signals of energy state, the modulation of Dm
665 activity appears to be primarily driven by neuronal inputs.

666 NPY containing neurons of the EN and periventricular hypothalamus also project to
667 the Dm. Thus, the Dm neurons could function as a common substrate for orexic and
668 anorexic inputs and their activity could be dynamically tuned to the prevailing energy
669 states. Indeed, both starvation and exogenous application of NPY to fed fish (low
670 levels of endogenous NPY) led to a reduction in Dm activity with a concomitant
671 increase in the feeding drive.

672 Our investigation reveals that NPY opposes CART-mediated elevation of NR1
673 phosphorylation and consequent increase in Dm activity and anorexia by reducing

674 cAMP production (thereby reducing PKA activation) and activating the phosphatase
675 calcineurin. Our observations are consistent with NPY-mediated activation of
676 calcineurin (Chen et al., 2005; Sajdyk et al., 2008) and calcineurin mediated
677 dephosphorylation of NR1(Choe et al., 2005). Further, NPY Y1R mediated reduction
678 in cAMP and PKA has been shown to decrease NMDA-mediated postsynaptic
679 currents (Molosh et al., 2013) in the neurons of the basolateral amygdala.

680 Our data suggest that Dm neurons are modulated by the opposing activities of CART
681 and NPY to achieve two distinct activity states (Fig. 8 E). Dm neurons, in zebrafish,
682 may represent “second order” neurons, immediately downstream of the
683 interoceptive, “first order” population in the hypothalamus and EN. While our
684 experiments are unable to distinguish whether the same individual neurons respond
685 differentially to CART and NPY, the tight correlation of Dm activity with alterations in
686 food intake behaviour suggest a pivotal role for Dm neurons in regulating energy
687 homoeostasis (Fig. 8 E). A major limitation in delineating CART function has been
688 the lack of well characterised receptors and selective pharmacology. This drawback
689 has limited our analysis of Dm neurons. However, collateral evidence from the
690 gustatory systems underscores the role of Dm in food intake. In a range of teleosts,
691 the preglomerular tertiary gustatory nucleus is reciprocally connected to the Dm
692 (Kanwal et al., 1988; Kato et al., 2012). Though the downstream targets of the Dm
693 relevant to the feeding drive are unknown, it appears CART/NPY activities modulate
694 the responsiveness of the Dm to glutamatergic inputs to release or inhibit food
695 intake.

696 The Dm is considered to be homologous to the mammalian amygdaloid complex
697 (Wullimann and Mueller, 2004; Porter and Mueller, 2020). Several recent reports
698 identify the mammalian amygdalar complex in the regulation of feeding behaviours

699 (Padilla et al., 2016; Kim et al., 2017; Izadi and Radahmadi, 2021). Consistent with
700 our findings, the amygdala receives projections from both the NPY and CART
701 neurons of the hypothalamic Arc (Hwang and Lee, 2018) and employs NPY Y1
702 mediated signalling to increase the food intake (Padilla et al., 2016). Additionally,
703 projections from dopamine receptor-positive neurons in prefrontal cortex are known
704 to activate medial BLA to increase food intake (Land et al., 2014). The amygdala is
705 also involved in hindbrain satiety circuits, where PKC-δ+ neurons in the central
706 amygdala (CeA) integrate multiple anorexigenic signals to inhibit food intake (Cai et
707 al., 2014). Conversely, Htr2a+ neurons of the CeA have been shown to stimulate
708 food intake (Douglass et al., 2017). In addition, several anorexigenic
709 neuromodulators, when administered to the CeA have been shown to affect food
710 intake (Fekete et al., 2007; Beckman et al., 2009; Kovács et al., 2012). A recent
711 study has identified appetitive information specific projections from the BLA to the
712 CeA and isolated specific CeA subpopulations that differentially mediate fear
713 processing and feeding-associated behaviours (Kim et al., 2017).

714 While the microcircuitry and the diversity of neuronal subtypes in the zebrafish Dm
715 remain unknown, the feeding regulation-associated CART/NPY-responsive neurons
716 could be distinct from those processing emotions. Consistent with this, no difference
717 in anxiety-like behaviours was seen in fish under fed and starved states or treated
718 with either of the neuropeptides (Fig. S2). The CART/NPY-responsive neurons are a
719 subpopulation restricted to a specific region of the Dm - starting at the level of the
720 anterior commissure and extending 250 μm rostrally (Fig. 2 G-I). Identification of
721 neuronal subtypes within the Dm and development of intersectional genetics will be
722 critical in characterising the CART/NPY-responsive microcircuits in the future.

723 This study investigates neural mechanisms mediating the opposing activities of the
724 neuropeptides CART and NPY in regulating the feeding drive in zebrafish and
725 identifies plasticity in a group of neurons in the zebrafish forebrain. CART and NPY
726 inputs converge on Dm neurons to antagonistically modulate NMDAR function,
727 resulting in an energy state-dependent alteration in glutamatergic neurotransmission
728 that is tightly correlated with the behavioural switch in food intake.

729

730 **REFERENCES**

731 Abercrombie, M. (1946). Estimation of nuclear population from microtome sections.
732 Anat. Rec. *94*, 239–247.

733 Akash, G., Kaniganti, T., Tiwari, N.K., Subhedar, N.K., and Ghose, A. (2014).
734 Differential distribution and energy status-dependent regulation of the four CART
735 neuropeptide genes in the zebrafish brain. J. Comp. Neurol. *522*, 2266–2285.

736 Andermann, M.L., and Lowell, B.B. (2017). Toward a Wiring Diagram Understanding
737 of Appetite Control. Neuron *95*, 757–778.

738 Aoki, T., Kinoshita, M., Aoki, R., Agetsuma, M., Aizawa, H., Yamazaki, M.,
739 Takahoko, M., Amo, R., Arata, A., Higashijima, S. ichi, et al. (2013). Imaging of
740 neural ensemble for the retrieval of a learned behavioral program. Neuron *78*, 881–
741 894.

742 Atasoy, D., and Sternson, S.M. (2016). Functional and Anatomical Dissection of
743 Feeding Circuits. Neuroendocrinol. Appet. 112–133.

744 Beckman, T.R., Shi, Q., Levine, A.S., and Billington, C.J. (2009). Amygdalar opioids
745 modulate hypothalamic melanocortin-induced anorexia. Physiol. Behav. *96*, 568–
746 573.

747 Betley, J.N., and Sternson, S.M. (2015). Applying the Brakes: When to Stop Eating.
748 Neuron *88*, 440–441.

749 Cai, H., Haubensak, W., Anthony, T.E., and Anderson, D.J. (2014). Central
750 amygdala PKC-δ+ neurons mediate the influence of multiple anorexigenic signals.
751 Nat. Neurosci. *17*, 1240–1248.

752 Carter, M.E., Soden, M.E., Zweifel, L.S., and Palmiter, R.D. (2013). Genetic
753 identification of a neural circuit that suppresses appetite. Nature *503*, 111–114.

754 Chen, B.S., and Roche, K.W. (2007). Regulation of NMDA receptors by
755 phosphorylation. Neuropharmacology *53*, 362–368.

756 Chen, M., Li, X., Dong, Q., Li, Y., and Liang, W. (2005). Neuropeptide Y induces

757 cardiomyocyte hypertrophy via calcineurin signaling in rats. Regul. Pept. *125*, 9–15.

758 Chen, Y., Lin, Y.C., Kuo, T.W., and Knight, Z.A. (2015). Sensory Detection of Food
759 Rapidly Modulates Arcuate Feeding Circuits. Cell *160*, 829–841.

760 Chen, Y., Lin, Y., Zimmerman, C.A., Essner, R.A., and Knight, Z.A. (2016). Hunger
761 neurons drive feeding through a sustained , positive reinforcement signal. 1–21.

762 Chiu, H.Y., Lin, H.H., and Lai, C.C. (2010). Cocaine- and amphetamine-regulated
763 transcript (CART) peptide activates ERK pathways via NMDA receptors in rat spinal
764 cord dorsal horn in an age-dependent manner. Regul. Pept. *164*, 90–96.

765 Choe, E.S., Shin, E.H., and Wang, J.Q. (2005). Inhibition of protein phosphatase 2B
766 upregulates serine phosphorylation of N-methyl-d-aspartate receptor NR1 subunits
767 in striatal neurons in vivo. Neurosci. Lett. *384*, 38–43.

768 Crespo, C.S., Cachero, A.P., Jiménez, L.P., Barrios, V., and Ferreiro, E.A. (2014).
769 Peptides and food intake. Front. Endocrinol. (Lausanne). *5*, 1–13.

770 Dietrich, M.O., and Horvath, T.L. (2013). Hypothalamic control of energy balance :
771 insights into the role of synaptic plasticity. Trends Neurosci. *36*, 65–73.

772 Doods, H.N., Wienen, W., Entzeroth, M., Rudolf, K., Eberlein, W., Engel, W., and
773 Wieland, H.A. (1995). Pharmacological characterization of the selective nonpeptide
774 neuropeptide Y Y1 receptor antagonist BIBP 3226. J. Pharmacol. Exp. Ther. *275*,
775 136–142.

776 Douglass, A.M., Kucukdereli, H., Ponserre, M., Markovic, M., Gründemann, J.,
777 Strobel, C., Alcala Morales, P.L., Conzelmann, K.K., Lüthi, A., and Klein, R. (2017).
778 Central amygdala circuits modulate food consumption through a positive-valence
779 mechanism. Nat. Neurosci. *20*, 1384–1394.

780 Elbaz, I., Yelin-Bekerman, L., Nicenboim, J., Vatine, G., and Appelbaum, L. (2012).
781 Genetic ablation of hypocretin neurons alters behavioral state transitions in
782 zebrafish. J. Neurosci. *32*, 12961–12972.

783 Ezcurra, X.M., Walker, X.D.S., Beets, I., Swoboda, X.P., and Schafer, W.R. (2016).
784 Neuropeptidergic Signaling and Active Feeding State Inhibit Nociception in

785 Caenorhabditis elegans. *36*, 3157–3169.

786 Farzi, A., Lau, J., Ip, C.K., Qi, Y., Shi, Y.C., Zhang, L., Tasan, R., Sperk, G., and
787 Herzog, H. (2018). Arcuate nucleus and lateral hypothalamic cart neurons in the
788 mouse brain exert opposing effects on energy expenditure. Elife *7*, 1–27.

789 Fekete, É.M., Bagi, É.E., Tóth, K., and Lénárd, L. (2007). Neuromedin C
790 microinjected into the amygdala inhibits feeding. Brain Res. Bull. *71*, 386–392.

791 Fenselau, H., Campbell, J.N., Verstegen, A.M.J., Madara, J.C., Xu, J., Shah, B.P.,
792 Resch, J.M., Yang, Z., Mandelblat-cerf, Y., Livneh, Y., et al. (2017). A rapidly acting
793 glutamatergic ARC → PVH satiety circuit postsynaptically regulated by a -MSH. *20*.

794 Flavell, S.W., Pokala, N., Macosko, E.Z., Albrecht, D.R., Larsch, J., and Bargmann,
795 C.I. (2013). Serotonin and the neuropeptide PDF initiate and extend opposing
796 behavioral states in C. Elegans. Cell *154*, 1023–1035.

797 Flavell, S.W., Raizen, D.M., and You, Y.J. (2020). Behavioral states. Genetics *216*,
798 315–332.

799 Forlano, P.M., and Cone, R.D. (2007). Conserved neurochemical pathways involved
800 in hypothalamic control of energy homeostasis. J. Comp. Neurol. *505*, 235–248.

801 Garfield, A.S., Li, C., Madara, J.C., Shah, B.P., Webber, E., Steger, J.S., Campbell,
802 J.N., Gavrilova, O., Lee, C.E., Olson, D.P., et al. (2015). A neural basis for
803 melanocortin-4 receptor–regulated appetite. Nat. Neurosci. *18*, 863–871.

804 Horvath, T.L., and Diano, S. (2004). The floating blueprint of hypothalamic feeding
805 circuits. Nat. Rev. Neurosci. *5*, 662–667.

806 Hwang, Y.G., and Lee, H.S. (2018). Neuropeptide Y (NPY) or cocaine- and
807 amphetamine-regulated transcript (CART) fiber innervation on central and medial
808 amygdaloid neurons that project to the locus coeruleus and dorsal raphe in the rat.
809 Brain Res. *1689*, 75–88.

810 Izadi, M.S., and Radahmadi, M. (2021). Overview of the central amygdala role in
811 feeding behaviour. Br. J. Nutr. 1–23.

812 Kaniganti, T., Deogade, A., Maduskar, A., Mukherjee, A., Guru, A., Subhedar, N.,
813 and Ghose, A. Sensitivity of olfactory sensory neurons to food cues is tuned to
814 nutritional states by Neuropeptide Y signaling. J. Neurochem.
815 (doi: 10.1111/jnc.15488).

816 Kanwal, J.S., Finger, T.E., and Caprio, J. (1988). Forebrain connections of the
817 gustatory system in ictalurid catfishes. J. Comp. Neurol. *278*, 353–376.

818 Kato, T., Yamada, Y., and Yamamoto, N. (2012). Ascending gustatory pathways to
819 the telencephalon in goldfish. J. Comp. Neurol. *520*, 2475–2499.

820 Kim, J., Zhang, X., Muralidhar, S., LeBlanc, S.A., and Tonegawa, S. (2017).
821 Basolateral to Central Amygdala Neural Circuits for Appetitive Behaviors. Neuron *93*,
822 1464-1479.e5.

823 Kovács, A., László, K., Gálosi, R., Tóth, K., Ollmann, T., Péczely, L., and Lénárd, L.
824 (2012). Microinjection of RFRP-1 in the central nucleus of amygdala decreases food
825 intake in the rat. Brain Res. Bull. *88*, 589–595.

826 Kristensen, P., Judge, M.E., Thim, L., Ribel, U., Christjansen, K.N., Wulff, B.S.,
827 Clausen, J.T., Jensen, P.B., Madsen, O.D., Vrang, N., et al. (1998). Hypothalamic
828 CART is a new anorectic peptide regulated by leptin. Nature *393*, 72–76.

829 Lan, J.Y., Skeberdis, V.A., Jover, T., Grooms, S.Y., Lin, Y., Araneda, R.C., Zheng,
830 X., Bennett, M. V, and Zukin, R.S. (2001). Protein kinase C modulates NMDA
831 receptor trafficking and gating. Nat. Neurosci. *4*, 382–390.

832 Land, B.B., Narayanan, N.S., Liu, R.-J., Gianessi, C.A., Brayton, C.E., M Grimaldi,
833 D., Sarhan, M., Guarnieri, D.J., Deisseroth, K., Aghajanian, G.K., et al. (2014).
834 Medial prefrontal D1 dopamine neurons control food intake. Nat. Neurosci. *17*, 248–
835 253.

836 Lau, J., and Herzog, H. (2014). CART in the regulation of appetite and energy
837 homeostasis. Front. Neurosci. *8*, 313.

838 Lee, S.H., and Dan, Y. (2012). Neuromodulation of Brain States. Neuron *76*, 209–
839 222.

840 Lin, H.H., Chiu, H.Y., and Lai, C.C. (2005). Potentiation of spinal N-methyl-D-
841 aspartate-mediated nociceptive transmission by cocaine-regulated and
842 amphetamine-regulated transcript peptide in rats. Neuroreport *16*, 253–257.

843 Liu, T., Kong, D., Shah, B.P., Ye, C., Koda, S., Saunders, A., Ding, J.B., Yang, Z.,
844 Sabatini, B.L., and Lowell, B.B. (2012). Fasting Activation of AgRP Neurons
845 Requires NMDA Receptors and Involves Spinogenesis and Increased Excitatory
846 Tone. Neuron *73*, 511–522.

847 Loh, K., Herzog, H., and Shi, Y.C. (2015). Regulation of energy homeostasis by the
848 NPY system. Trends Endocrinol. Metab. *26*, 125–135.

849 Mathieu, M., Tagliafierro, G., Bruzzone, F., and Vallarino, M. (2002). Neuropeptide
850 tyrosine-like immunoreactive system in the brain, olfactory organ and retina of the
851 zebrafish, Danio rerio, during development. Dev. Brain Res. *139*, 255–265.

852 Molosh, A.I., Sajdyk, T.J., Truitt, W.A., Zhu, W., Oxford, G.S., and Shekhar, A.
853 (2013). NPY Y1 Receptors Differentially Modulate GABAA and NMDA Receptors via
854 Divergent Signal-Transduction Pathways to Reduce Excitability of Amygdala
855 Neurons. Neuropsychopharmacology *38*, 1352–1364.

856 Mukherjee, A., Subhedar, N.K., and Ghose, A. (2012). Ontogeny of the cocaine- and
857 amphetamine-regulated transcript (CART) neuropeptide system in the brain of
858 zebrafish, Danio rerio. J. Comp. Neurol. *520*, 770–797.

859 Nadim, F., and Bucher, D. (2014). Neuromodulation of neurons and synapses. Curr.
860 Opin. Neurobiol. *29*, 48–56.

861 Neyens, D., Zhao, H., Huston, N.J., Wayman, G.A., Ritter, R.C., and Appleyard, S.M.
862 (2020). Leptin sensitizes NTS neurons to vagal input by increasing postsynaptic
863 NMDA receptor currents. J. Neurosci. *40*, 7054–7064.

864 Nishio, S.-I., Gibert, Y., Berekelya, L., Bernard, L., Brunet, F., Guillot, E., Le Bail, J.-
865 C., Sánchez, J.A., Galzin, A.M., Triqueneaux, G., et al. (2012). Fasting Induces
866 CART Down-Regulation in the Zebrafish Nervous System in a Cannabinoid Receptor
867 1-Dependent Manner. Mol. Endocrinol. *26*, 1316–1326.

868 Padilla, S.L., Qiu, J., Soden, M.E., Sanz, E., Nestor, C.C., Barker, F.D., Quintana, A.,
869 Zweifel, L.S., Rønnekleiv, O.K., Kelly, M.J., et al. (2016). Agouti-related peptide
870 neural circuits mediate adaptive behaviors in the starved state. Nat. Neurosci. *19*,
871 734–741.

872 van den Pol, A.N. (2012). Neuropeptide Transmission in Brain Circuits. Neuron *76*,
873 98–115.

874 Porter, B.A., and Mueller, T. (2020). The Zebrafish Amygdaloid Complex –
875 Functional Ground Plan, Molecular Delineation, and Everted Topology. Front.
876 Neurosci. *14*.

877 Rale, A., Shendye, N., Bodas, D.S., Subhedar, N., and Ghose, A. (2017). CART
878 neuropeptide modulates the extended amygdalar CeA-vBNST circuit to gate
879 expression of innate fear. Psychoneuroendocrinology *85*, 69–77.

880 Randlett, O., Wee, C.L., Naumann, E.A., Nnaemeka, O., Schoppik, D., Fitzgerald,
881 J.E., Portugues, R., Lacoste, A.M.B., Riegler, C., Engert, F., et al. (2015). Whole-
882 brain activity mapping onto a zebrafish brain atlas. Nat. Methods *12*, 1039–1046.

883 Resch, J.M., Maunze, B., Phillips, K.A., and Choi, S. (2014). Inhibition of food intake
884 by PACAP in the hypothalamic ventromedial nuclei is mediated by NMDA receptors.
885 Physiol. Behav. *133*, 230–235.

886 Root, C.M., Ko, K.I., Jafari, A., and Wang, J.W. (2011). Presynaptic facilitation by
887 neuropeptide signaling mediates odor-driven food search. Cell *145*, 133–144.

888 Sainsbury, A., and Zhang, L. (2010). Role of the arcuate nucleus of the
889 hypothalamus in regulation of body weight during energy deficit. Mol. Cell.
890 Endocrinol. *316*, 109–119.

891 Sajdyk, T.J., Johnson, P.L., Leitermann, R.J., Fitz, S.D., Dietrich, A., Morin, M.,
892 Gehlert, D.R., Urban, J.H., and Shekhar, A. (2008). Neuropeptide Y in the Amygdala
893 Induces Long-Term Resilience to Stress-Induced Reductions in Social Responses
894 But Not Hypothalamic-Adrenal-Pituitary Axis Activity or Hyperthermia. J. Neurosci.
895 *28*, 893–903.

896 Singh, A., de Araujo, A.M., Krieger, J.P., Vergara, M., Ip, C.K., and de Lartigue, G.
897 (2021). Demystifying functional role of cocaine- and amphetamine-related transcript
898 (CART) peptide in control of energy homeostasis: A twenty-five year expedition.
899 Peptides *140*, 170534.

900 Skeberdis, V.A., Chevaleyre, V., Lau, C.G., Goldberg, J.H., Pettit, D.L., Suadicani,
901 S.O., Lin, Y., Bennett, M.V.L., Yuste, R., Castillo, P.E., et al. (2006). Protein kinase A
902 regulates calcium permeability of NMDA receptors. Nat. Neurosci. *9*, 501–510.

903 Stanley, B.G., Urstadt, K.R., Charles, J.R., and Kee, T. (2011). Glutamate and GABA
904 in lateral hypothalamic mechanisms controlling food intake. Physiol. Behav. *104*, 40–
905 46.

906 Sternson, S.M. (2013). Hypothalamic survival circuits: Blueprints for purposive
907 behaviors. Neuron *77*, 810–824.

908 Subhedar, N., Barsagade, V.G., Singru, P.S., Thim, L., and Clausen, J.T. (2011).
909 Cocaine- and Amphetamine-Regulated Transcript Peptide (CART) in the
910 Telencephalon of the Catfish , Clarias gariepinus : Distribution and Response to
911 Fasting , 2-Deoxy-D-glucose , Glucose , Insulin , and Leptin Treatments. *1300*,
912 1281–1300.

913 Subhedar, N.K., Nakhate, K.T., Upadhya, M.A., and Kokare, D.M. (2014). CART in
914 the brain of vertebrates: Circuits, functions and evolution. Peptides *54*, 108–130.

915 Tong, C.-K., Pan, M.-P., and Chang, Y.-C. (1992). Characterization of l-glutamate
916 and kainate binding sites in the brain of a freshwater fish, Telapilia monsanbica.
917 Neuroscience *49*, 237–246.

918 Turner, K.J., Hawkins, T.A., Yáñez, J., Anadón, R., Wilson, S.W., and Folgueira, M.
919 (2016). Afferent Connectivity of the Zebrafish Habenulae. Front. Neural Circuits *10*,
920 30.

921 Wright, J., Campos, C., Herzog, T., Covasa, M., Czaja, K., and Ritter, R.C. (2011).
922 Reduction of food intake by cholecystokinin requires activation of hindbrain NMDA-
923 type glutamate receptors. Am. J. Physiol. - Regul. Integr. Comp. Physiol. *301*, 448–
924 455.

Wullimann, M.F., and Mueller, T. (2004). Erratum: Teleostean and mammalian forebrains contrasted: Evidence from genes to behavior (Journal of Comparative Neurology (2004) 475 (143-162)). J. Comp. Neurol. *478*, 427–428.

Yamamoto, N., and Ito, H. (2005). Fiber connections of the anterior preglomerular nucleus in cyprinids with notes on telencephalic connections of the preglomerular complex. J. Comp. Neurol. *491*, 212–233.

Yáñez, J., Souto, Y., Piñeiro, L., Folgueira, M., and Anadón, R. (2017). Gustatory and general visceral centers and their connections in the brain of adult zebrafish: a carbocyanine dye tract-tracing study. J. Comp. Neurol. *525*, 333–362.

Yang, Y., Atasoy, D., and Sternson, S. (2011). Flip-flop memory circuit uses a synaptic AMPK-dependent positive feedback loop and is switched by hunger state. Appetite *57*, S47.

Yokobori, E., Azuma, M., Nishiguchi, R., Kang, K.S., Kamijo, M., Uchiyama, M., and Matsuda, K. (2012). Neuropeptide Y Stimulates Food Intake in the Zebrafish, Danio rerio. J. Neuroendocrinol. *24*, 766–773.

Yokogawa, T., Marin, W., Faraco, J., Pézeron, G., Appelbaum, L., Zhang, J., Rosa, F., Mourrain, P., and Mignot, E. (2007). Characterization of sleep in zebrafish and insomnia in hypocretin receptor mutants. PLoS Biol. *5*, 2379–2397.

Zhang, L., Hernandez-Sanchez, D., and Herzog, H. (2019). Regulation of Feeding-Related Behaviors by Arcuate Neuropeptide Y Neurons. Endocrinology *160*, 1411–1420.

ETHICS APPROVAL

All protocols used in this study were approved by Institutional Animal Ethics Committee of IISER Pune.

AVAILABILITY OF DATA AND MATERIAL

All data generated or analysed during this study are included in this published article. The raw data are available from the corresponding author on reasonable request.

CONFLICT OF INTEREST

The authors declare that they have no conflict of interest.

FUNDING

The study was supported by intramural support from IISER Pune to A.G. and a grant from the Department of Biotechnology, Govt. of India (BT/PR26241/GET/119/244/2017) to A.G.. D.B. was support by a fellowship from IISER Pune and A.M. was supported by a fellowship from the Council for Scientific and Industrial Research. The National Facility for Gene Function in Health and Disease (NFGFHD) at IISER Pune is supported by the Department of Biotechnology, Govt. of India (BT/INF/22/SP17358/2016).

AUTHOR CONTRIBUTIONS

Conceptualization: D.B., A.M., N.S. and A.G.; Investigation and formal analysis: D.B., A.M. and T.K.; Generation of preliminary data: D.W. and A.B.; Writing – original draft: D.B., A.M. and A.G.; Writing – review and editing: D.B., A.M., N.S. and A.G.; Funding Acquisition: A.G.. All authors gave final approval for publication and agree to be held accountable for the work performed therein.

ACKNOWLEDGMENTS

The authors thank Dr. G. Deshpande, Princeton University, Dr. S. Rath, IISER Pune and Dr. R. Rajan, IISER Pune for their critical reading of this manuscript and discussions. The Tg(NeuroD:GCaMP6f) line was a gift from Dr. V. Thirumalai, NCBS, Bengaluru. N. Tiwari, IISER Pune is acknowledged for contributing to the development of the feeding assay. The authors acknowledge the IISER Pune Microscopy Facility and the National Facility for Gene Function in Health and Disease (NFGFHD) at IISER Pune for access to equipment and infrastructure.

985 **FIGURE LEGENDS**

986 **Figure 1. CART neuropeptide regulates satiety in adult zebrafish.**

987 **(A)** The feeding drive as indicated by the cumulative number of biting attempts made
988 by fed and starved animals in 15 min bins (N=6 animals per group). **(B)**The
989 cumulative number of biting attempts made by starved fish intracerberoventicularly
990 injected with either vehicle or CART peptide (N=6 animals per group). **(C)**The
991 cumulative number of biting attempts made by starved fish icv injected with either
992 vehicle, glucose, CART antibodies or coinjected with immunoneutralising CART
993 antibodies (CART Ab) along with glucose (N= 5 for vehicle control and CART Ab
994 treated animals and N=6 for glucose and CART Ab + glucose treated animals). Data
995 are represented as cumulative biting attempts in 15 min bins over a 1-hour period
996 and compared using two-way ANOVA, with Bonferroni's post-hoc analysis for
997 significance in comparison with the glucose treated starved fish (error bars represent
998 ± SEM; ns, not significant; **p<0.01, ***p<0.001).

999

1000 **Figure 2. CART neuropeptide and satiety increases the activity of the**
1001 **dorsomedial telencephalon (Dm) neurons.**

1002 **(A,B)** Representative micrographs of Dm region from the transverse sections of the
1003 telencephalon showing p-ERK immunoreactive (p-ERK-ir) cells in starved fish icv
1004 injected with either vehicle or CART peptide. **(C)** The number of p-ERK-ir cells in Dm
1005 in starved fish icv injected with either vehicle or CART. The data are compared using
1006 the unpaired t-test with Welch's correction (N=6 animals per group; **p<0.01). **(D,E)**
1007 representative micrographs of Dm region from the transverse sections of the
1008 telencephalon showing p-ERK-ir cells under starved and fed conditions. **(F)** The

1009 number of p-ERK-ir cells in Dm under starved and fed states. The data are
1010 compared using the unpaired t-test with Welch's correction (N=6 animals per group).
1011 (**p<0.01, ***p<0.001). Scale bar: 50 μm. **(G)** The top view of zebrafish
1012 telencephalon with shaded region (dark red) indicating the entire dorsomedial
1013 telencephalon. The area bounded by dotted lines within dorsomedial telencephalon
1014 (light red) shows differential activity upon CART treatment and under fed/starved
1015 conditions. We refer to this subregion as Dm for the purposes of this study. **(H)** Side
1016 view of zebrafish brain with dark red area marking entire dorsomedial telencephalon.
1017 The region of our interest – within dorsomedial telencephalon - Dm (light red) is
1018 marked by dotted lines (a: marks the rostral limit of the region which shows
1019 differential activity; b: marks the plane of section shown in I; c: marks the caudal limit
1020 at the level of the anterior commissure (ac); the distance from a to c is ~250 μm). **(I)**
1021 A transverse section of telencephalon with the Dm region marked in light red colour.
1022 [ac, anterior commissure; Dp, posterior zone of dorsal telencephalon; EN,
1023 entopeduncular nucleus; Hy, hypothalamus; Ha, habenula; IOP, integrative olfactory
1024 pallium; MP, medial pallium; nLOT- nucleus of the lateral olfactory tract; OB,
1025 olfactory bulb; PMPa, posteromedial pallial nucleus; Sy, sulcus yipsiloniformis; TeO,
1026 optic tectum; Vd, dorsal nucleus of ventral telencephalic area; Vv, ventral nucleus of
1027 ventral telencephalic area]

1028

1029 **Figure 3. NMDAR signalling is necessary for CART-induced anorexia and**
1030 **increased activation of Dm neurons.**

1031 **(A)** The cumulative number of biting attempts made by starved zebrafish icv injected
1032 with either vehicle, CART peptide, AP5 or coinjected with AP5 and CART peptide.
1033 (N=6 animals per group). Data are represented as cumulative biting attempts in 15

1034 min bins over a 1-hour period and compared using two-way ANOVA, with
1035 Bonferroni's post-hoc analysis (error bars represent ±SEM; **p<0.01, ***p<0.001).
1036 **(B)** The number of p-ERK-ir cells in starved fish icv injected with either vehicle,
1037 CART, AP5 or coinjection of AP5 along with CART. The data are compared using
1038 two-way ANOVA, with Bonferroni's post-hoc analysis for significance in comparison
1039 with the CART treated starved fish (N=6 animals per group; ***p<0.001).

1040

1041 **Figure 4. CART-induced anorexia and activation of Dm neurons require PKA**
1042 **and PKC activity.**

1043 **(A)** The cumulative number of biting attempts made by starved fish icv injected with
1044 either vehicle, CART, PKAi or coinjection of PKAi along with CART. (N=6 animals
1045 per group). Data are represented as cumulative biting attempts in 15 min bins over a
1046 1-hour period and compared using two-way ANOVA, with Bonferroni's post-hoc
1047 analysis for significance in comparison with the CART treated starved fish (error bars
1048 represent ±SEM; ns, not significant; ***p<0.001, **p<0.01). **(B)** The number of p-
1049 ERK-ir cells in starved fish icv injected with either vehicle, CART peptide, PKAi or
1050 coinjected with PKAi and CART peptide. Data are compared using two-way ANOVA,
1051 with Bonferroni's post-hoc analysis for significance in comparison with the CART
1052 treated starved fish (N=6 animals per group; ***p< 0.001, **p<0.01). **(C)** The
1053 cumulative number of biting attempts made by starved fish icv injected with either
1054 vehicle, CART peptide, PKCi or coinjected with PKCi and CART peptide. (N=6
1055 animals per group). Data are represented as cumulative biting attempts in 15 min
1056 bins over a 1-hour period and compared using two-way ANOVA, with Bonferroni's
1057 post-hoc analysis for significance in comparison with the CART treated starved fish
1058 (error bars represent ±SEM; ***p<0.001, **p<0.01). **(D)** The number of p-ERK-ir cells

1059 in starved fish icv injected with either vehicle, CART, PKCi or coinjection of PKCi
1060 along with CART. The data are compared using two-way ANOVA, with Bonferroni's
1061 post-hoc analysis for significance in comparison with the CART treated starved fish
1062 (N=6; ***p< 0.001). **(E,F)** representative micrographs of one lobe of the Dm region
1063 from the transverse sections of the telencephalon showing phosphoNR1 (Ser-897)
1064 (pNR1) immunoreactivity in starved fish icv injected with either CART peptide or co-
1065 injected with PKAi and PKCi along with CART peptide. **(G)** Quantification of mean
1066 pNR1 intensity per neuron (au: arbitrary units) in the Dm of starved fish icv injected
1067 with either vehicle and CART or coinjected with PKAi and PKCi along with CART
1068 peptideThe data were compared using unpaired t-test with Welch's correction
1069 (12253 cells in vehicle +CART group and 12015 cells in PKAi + PKCi + CART group;
1070 N=3 animals per group; ***p< 0.001. Scale bar: 50 μm.)

1071

1072 **Figure 5. CART treatment enhances NMDAR function resulting in increased**
1073 **sensitivity of Dm neurons to glutamate.**

1074 **(A)** A timeline of the experimental protocol followed for all calcium imaging
1075 experiments using *ex-vivo* telencephalon preparations (details in Methods).
1076 Representative micrographs of neural activity (GCaMP6f fluorescence) in the Dm of
1077 vehicle (**B**) and CART peptide (**B'**) injected Tg(NeuroD:GCaMP6f**)** transgenic
1078 animals following stimulation with glutamate for the same time. The ventricle is
1079 towards the top of the image and C and R indicate caudal and rostral directions,
1080 respectively. Scale bar: 50 μm. In all graphs **(C, F, I)**, the traces represent relative
1081 change in fluorescence intensity (ΔF/F0) across time. The dark line represents the
1082 mean and the dotted lines denote the standard error of mean. The shaded
1083 rectangular box indicates the duration of glutamate presentation. (**C**) The change in

1084 fluorescence intensity (ΔF/F0) of Dm neurons in starved fish treated with either
1085 CART peptide (blue trace) or vehicle (brown trace). **(D)** The maximum response
1086 (ΔF/F0) and **(E)** the extent of the total response – AUC (area under the curve) for Dm
1087 neurons in starved fish treated with either CART peptide or vehicle. The data were
1088 compared using t-test with Welch's correction. (N=6 telencephalons per group,
1089 **p<0.01). **(F)** The change in fluorescence intensity (ΔF/F0) of Dm neurons in starved
1090 fish treated with either CART peptide (blue trace) or coinjected with AP5 and CART
1091 peptide (brown trace). **(G)** The maximum response (ΔF/F0) and **(H)** the extent of the
1092 total response of Dm neurons in starved fish treated with either CART peptide or
1093 coinjected with AP5 and CART. The data were compared using t-test with Welch's
1094 correction (N= 5 for CART and N=6 for AP5+CART telencephalons, *p<0.05). **(I)** The
1095 change in fluorescence intensity (ΔF/F0) of Dm neurons in starved fish treated with
1096 either CART peptide (blue trace) or coinjected with PKAi and PKCi along with CART
1097 peptide (brown trace). **(J)** The maximum response (ΔF/F0) and **(K)** the extent of the
1098 total response of Dm neurons in starved fish treated with either CART peptide or
1099 coinjected with PKAi, PKCi along with CART peptide. The data were compared using
1100 the t-test with Welch's correction (N=6 telencephalons per group, **p<0.01).

1101

1102 **Figure 6. Activity of Dm neurons increases in response to glucose.**

1103 **(A)** A timeline of the experimental protocol followed for calcium imaging experiments
1104 using *ex-vivo* whole brain preparations (details in Methods) **(B)** The traces represent
1105 relative change in fluorescence intensity (ΔF/F0) over time in response to glutamate.
1106 The thicker line represents mean while the associated finer lines indicate ± SEM.
1107 The shaded rectangular box indicates the duration of glutamate presentation.
1108 Response of Dm neurons in *ex-vivo* whole brain samples post 30' incubation with

1109 glucose (dark blue trace; post-glucose) is substantial compared to pre-glucose
1110 treatment (dark brown trace). Control experiments showed no response of Dm
1111 neurons before (light brown; pre-control) and after (light blue; post-control) 30 min
1112 incubation in glucose-free media. **(C)** The maximum response (ΔF/F0) and **(D)** the
1113 extent of the total response of Dm neurons pre- and post- incubation with
1114 glucose/glucose-free media. The data were analysed using one-way ANOVA and
1115 Tukey's multiple comparisons test (N=5 brains in each group, ***p<0.001)**.**

1116

1117 **Figure 7. NPY promotes food intake and reduces the activation of Dm neurons.**

1118 **(A)** The cumulative number of biting attempts made by starved fish icv injected with
1119 either vehicle or BIBP3226 (N= 6; ***p<0.001). **(B)** The cumulative number of biting
1120 attempts made by fed fish icv injected with either vehicle or NPY (N=6; **p<0.01,
1121 ***p<0.001). Data are represented as cumulative biting attempts in 15 min bins over
1122 a 1-hour period and were compared using Two-way ANOVA, with Bonferroni's post-
1123 hoc analysis. **(C,D)** Representative micrographs of Dm region from the transverse
1124 sections across telencephalon showing p-ERK immunoreactive (p-ERK-ir) cells in
1125 fed fish icv injected with either vehicle or NPY **(E)** The number of p-ERK-ir cells in
1126 Dm of fed fish icv injected with either vehicle or NPY. The data were compared using
1127 unpaired t-test with Welch's correction (N=6; **p< 0.01). **(F,G)** representative
1128 micrographs of one lobe of Dm region from the transverse sections across
1129 telencephalon showing phosphoNR1 (pNR1) immunoreactivity in starved fish icv
1130 injected with either glucose or co-injected with NPY along with glucose **(H)**
1131 Quantification of mean pNR1 intensity per neuron (au: arbitrary units) in Dm in
1132 starved fish icv injected with either glucose or co-injected with NPY along with
1133 glucose. The data were compared using unpaired t-test with Welch's correction

1134 (12253 cells in vehicle+ glucose group and 11901 in NPY + glucose group; N=3;
1135 ***p< 0.001) [Scale bar 50 μm] **(I)** The traces represent relative change in
1136 fluorescence intensity (ΔF/F0) over time in response to 75 μM glutamate. The dark
1137 line represents mean ± SEM with the dotted lines denoting the limits for standard
1138 error. The coloured rectangular box indicates the duration for which glutamate was
1139 presented. The response of Dm neurons in starved fish ICV injected glucose (blue
1140 trace) and co-injected with NPY along with glucose (brown trace). **(J)** The max
1141 (ΔF/F0) as well as **(K)** AUC of response of Dm neurons in starved fish icv injected
1142 glucose compared with the starved fish co-injected with NPY along with glucose. The
1143 data were analysed using t-test with Welch's correction. (N=6 telencephalons per
1144 group, *p<0.05).

1145

1146 **Figure 8 NPY inhibits adenylyl cyclase and activates of calcineurin to promote**
1147 **food intake.**

1148 **(A)** The cumulative number of biting attempts made by fed fish icv injected with
1149 either vehicle, NPY, FK506 or co-injection of FK506 along with NPY. (N=5 animals
1150 per group). Data are represented as cumulative biting attempts in 15 min bins over a
1151 1-hour period and compared using Two-way ANOVA, with Bonferroni's post-hoc
1152 analysis for significance in comparison with the NPY treated fed fish(error bars
1153 represent ± SEM; *** p<0.001). **(B)** The number of p-ERK-ir cells in fed fish icv
1154 injected with either vehicle, NPY, FK506 or co-injection of FK506 along with NPY.
1155 Data were compared using Two-way ANOVA, with Bonferroni's post-hoc analysis for
1156 significance in comparison with the NPY treated fed fish (N=5; *** p< 0.001). **(C)** The
1157 cumulative number of biting attempts made by fed fishicv injected with either vehicle,
1158 NPY, Forskolin or co-injection of Forskolin along with NPY (N=5 animals per group).

1159 Data are represented as cumulative biting attempts in 15 min bins over a 1-hour
1160 period and were compared using Two-way ANOVA, with Bonferroni's post-hoc
1161 analysis for significance in comparison with the NPY treated fed fish (error bars
1162 represent ± SEM; *** $p<0.001$, *$p<0.05$). **(D)** The number of p-ERK-ir cells in fed fish
1163 icv injected with either vehicle, NPY, Forskolin or coinjection of Forskolin along with
1164 NPY. Data are compared using Two-way ANOVA, with Bonferroni's post-hoc
1165 analysis for significance in comparison with the NPY treated fed fish(N=5; ** $p<$
1166 0.01). **(E)** Schematic showing CART and NPY projections to Dm from interoceptive
1167 regions in zebrafish brain. [OB: olfactory bulb; EN: Entopeduncular nucleus; ac:
1168 anterior commissure; Ha: Habenula; Hy: Hypothalamus; TeO: Optic tectum] **(E')**
1169 Summary of modulatory changes induced by CART and NPY leading to a
1170 corresponding change in neural activity and food intake under fed and starved
1171 conditions, respectively. Under energy enriched conditions (Fed), CART signalling at
1172 the Dm is increased. CART activates PKA and PKC to increase the phosphorylation
1173 of NR1 subunit of NMDARs and thereby increases NMDAR activity in Dm neurons.
1174 CART mediated increase in Dm neuronal activity is correlated with a decrease in
1175 food intake in zebrafish. In contrast, under energy deprived conditions, NPY
1176 signalling at the Dm is increased. NPY acting via Y1R reduces PKA activity and
1177 activates calcineurin to decrease phosphorylation of NR1, in turn, decreasing
1178 NMDAR activity. NPY mediated reduction in Dm neuronal activity is correlated with
1179 increased food intake in zebrafish.

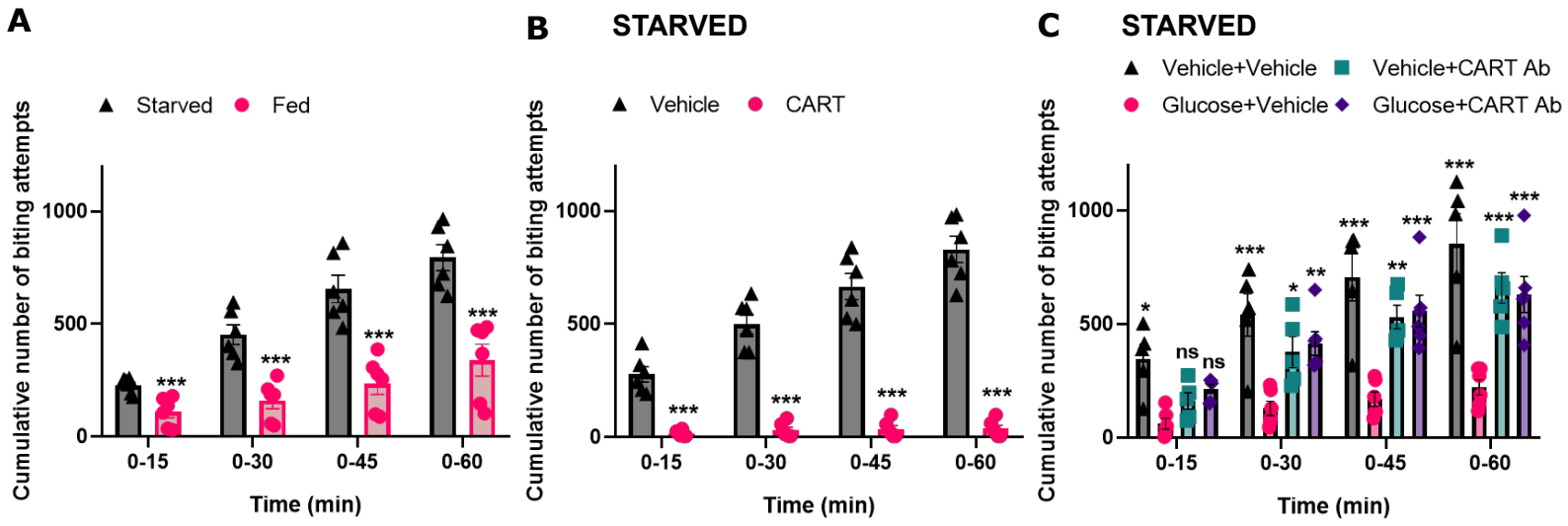
A
Starved
Fed
Cumulative number of biting attempts
1000
500
0
***
0-15
0-30
0-45
0-60
Time (min)
B
STARVED
Vehicle
CART
C
STARVED
Vehicle+Vehicle
Vehicle+CART Ab
Glucose+Vehicle
Glucose+CART Ab
ns
*
**

Figure 1

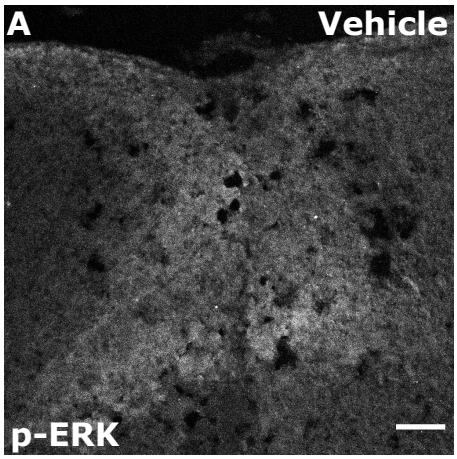
A
Vehicle
p-ERK

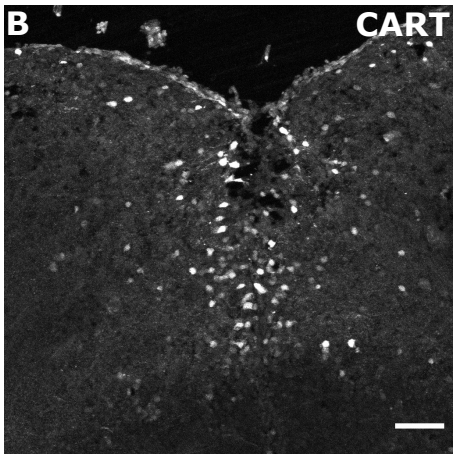
B
CART

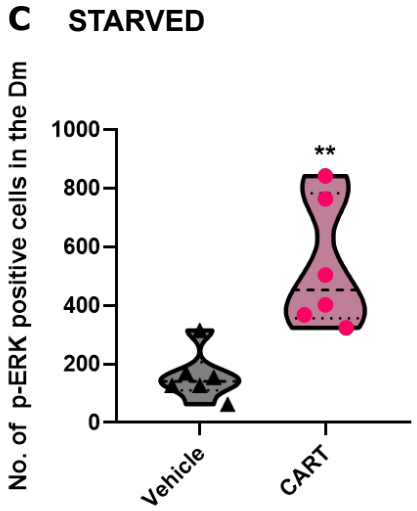
C
STARVED
No. of p-ERK positive cells in the Dm
1000
800
600
400
200
0
**
Vehicle
CART

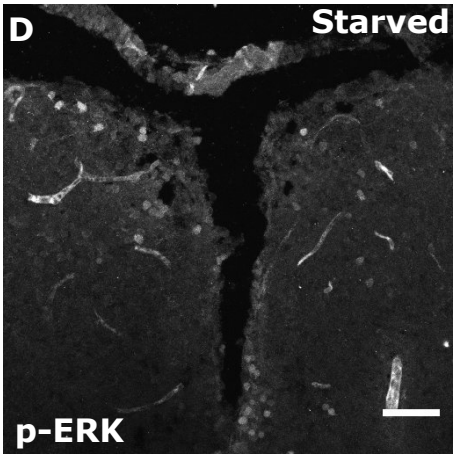
D
Starved
p-ERK

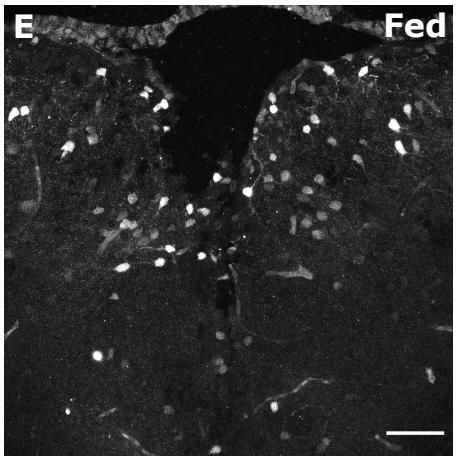
E
Fed

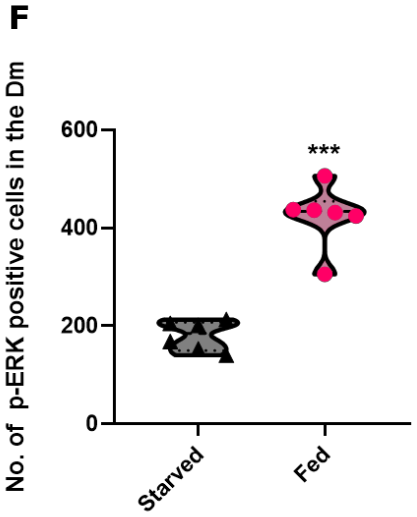
F
No. of p-ERK positive cells in the Dm
600
400
200
0
***
Starved
Fed

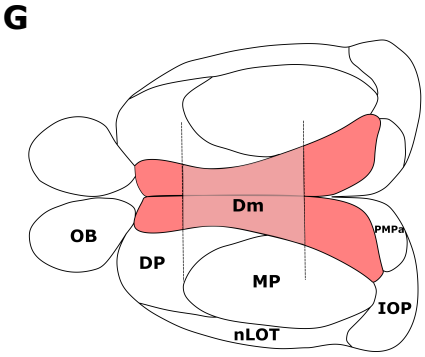
G
Dm
OB
DP
MP
PMPa
IOP
nLOT

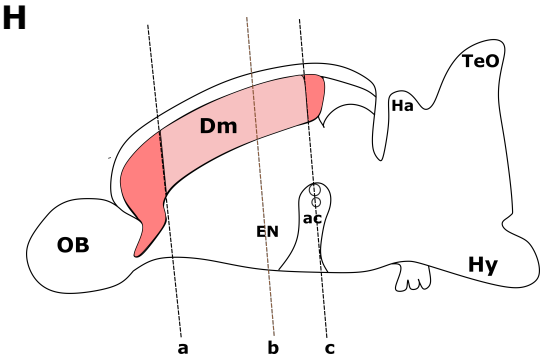
H
TeO
Ha
Dm
OB
EN
ac
Hy
a
b
c

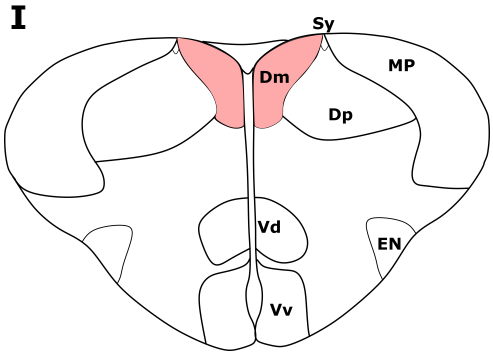
I
Sy
MP
Dm
Dp
Vd
EN
Vv

Figure 2

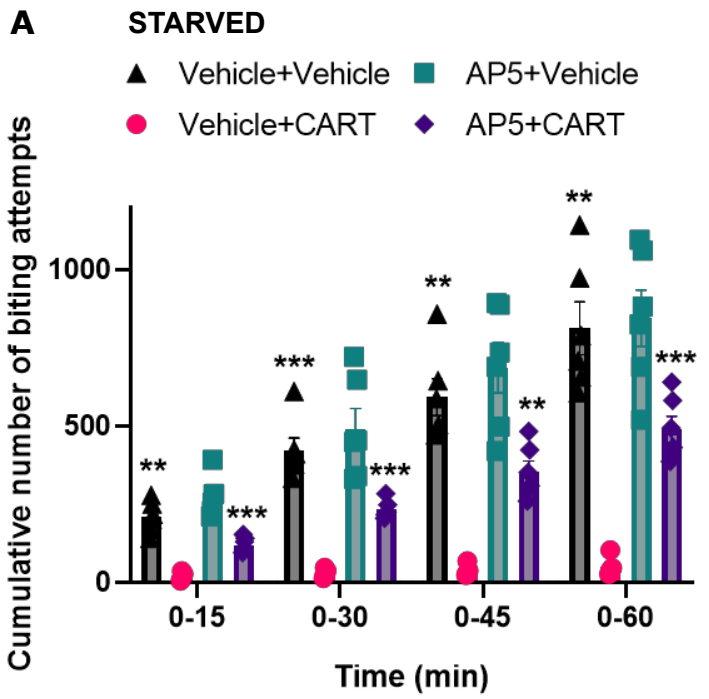
A
STARVED
Vehicle+Vehicle
AP5+Vehicle
Vehicle+CART
AP5+CART
Cumulative number of biting attempts
1000
500
0
**
***
***
**
***
**
**
***
0-15
0-30
0-45
0-60
Time (min)

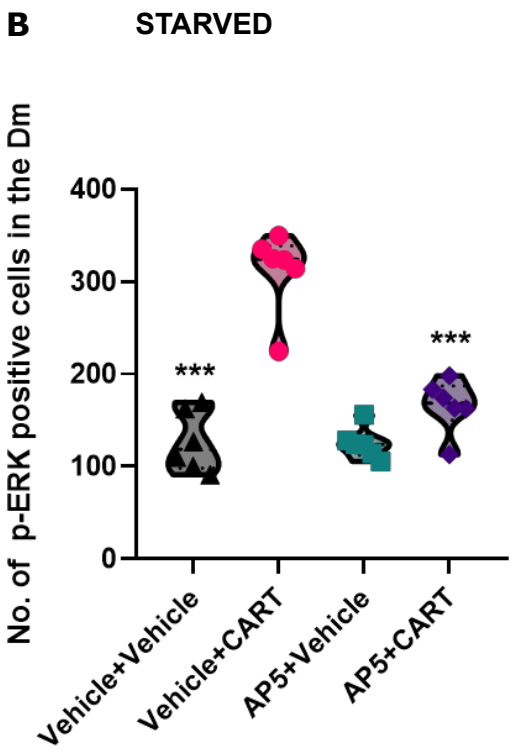
B
STARVED
No. of p-ERK positive cells in the Dm
400
300
200
100
0
***
***
Vehicle+Vehicle
Vehicle+CART
AP5+Vehicle
AP5+CART

Figure3

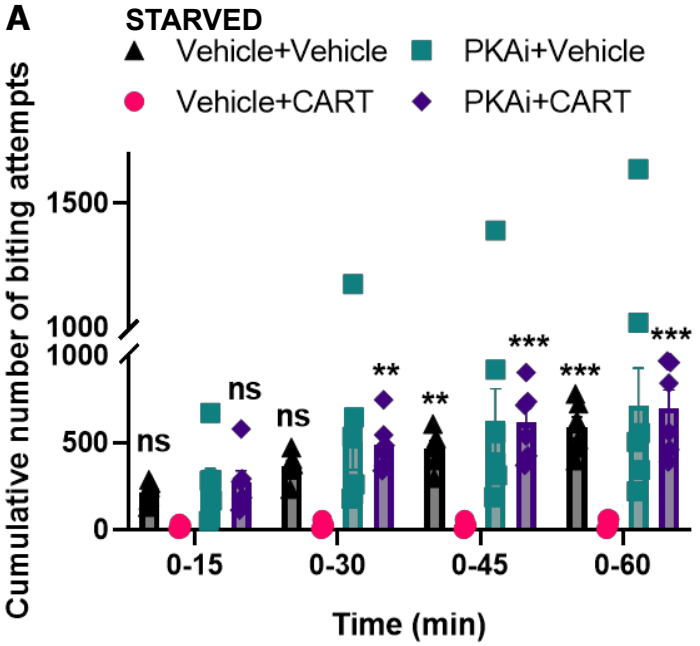
A
STARVED
Vehicle+Vehicle
PKAi+Vehicle
Vehicle+CART
PKAi+CART
Cumulative number of biting attempts
1500
1000
1000
500
0
ns
ns
ns
**
**
***
***
***
0-15
0-30
0-45
0-60
Time (min)

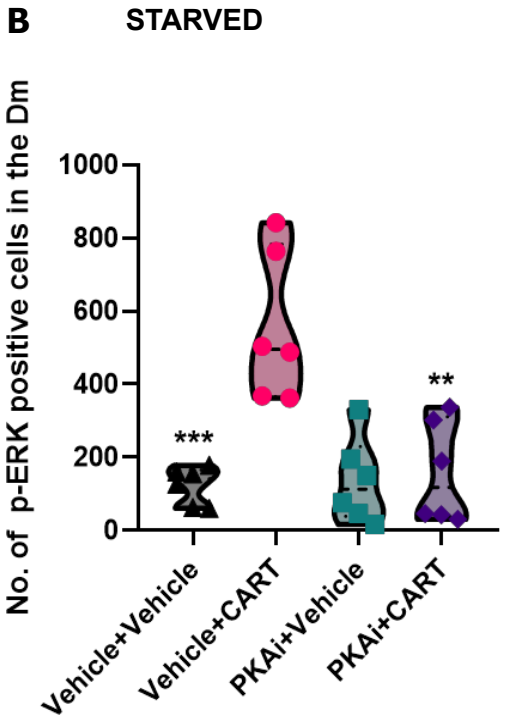
B
STARVED
No. of p-ERK positive cells in the Dm
1000
800
600
400
200
0
***
**
Vehicle+Vehicle
Vehicle+CART
PKAi+Vehicle
PKAi+CART

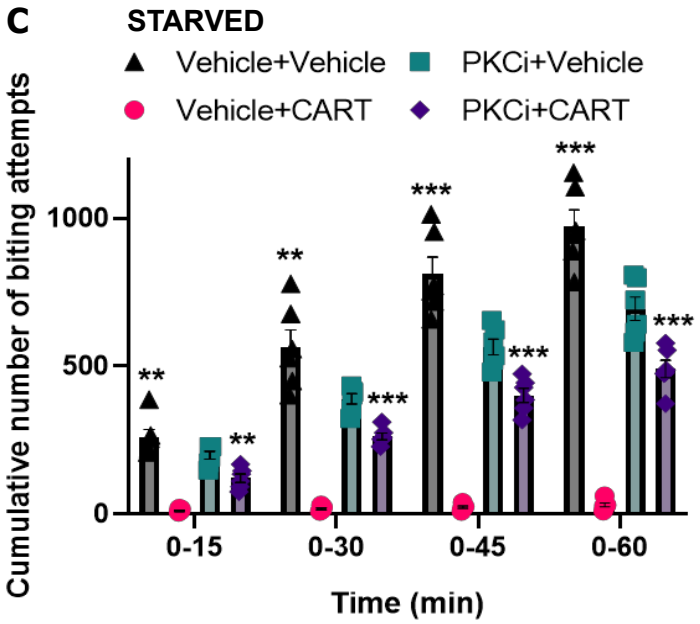
C
STARVED
Vehicle+Vehicle
PKCi+Vehicle
Vehicle+CART
PKCi+CART
Cumulative number of biting attempts
1000
500
0
**
**
**
***
***
***
***
***
0-15
0-30
0-45
0-60
Time (min)

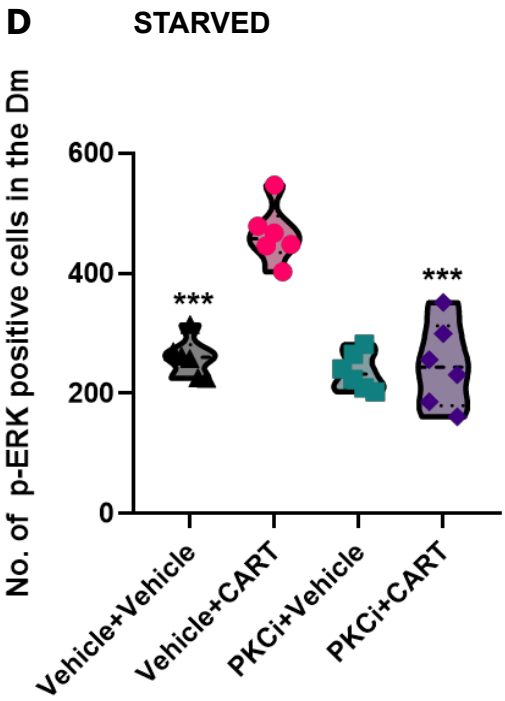
D
STARVED
No. of p-ERK positive cells in the Dm
600
400
200
0
***
***
Vehicle+Vehicle
Vehicle+CART
PKCi+Vehicle
PKCi+CART

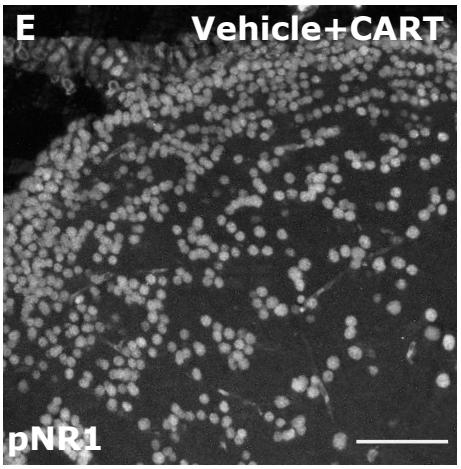
E
Vehicle+CART
pNR1

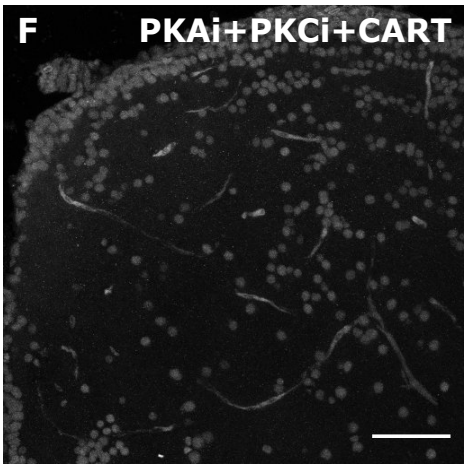
F
PKAi+PKCi+CART

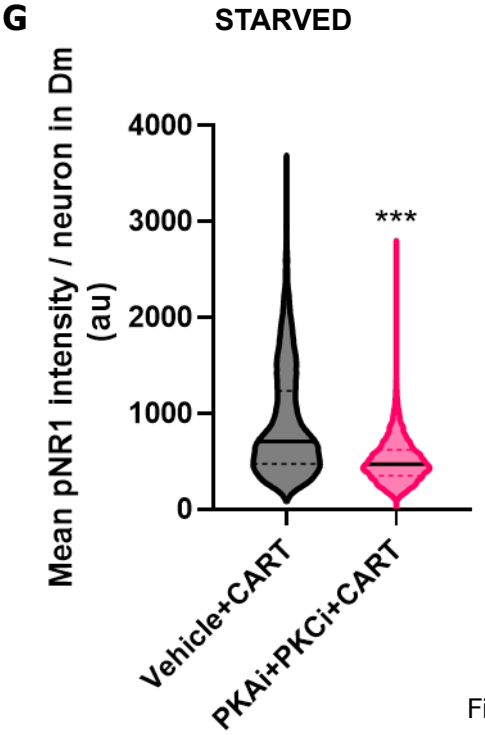
G
STARVED
Mean pNR1 intensity / neuron in Dm (au)
4000
3000
2000
1000
0
***
Vehicle+CART
PKAi+PKCi+CART

Figure4

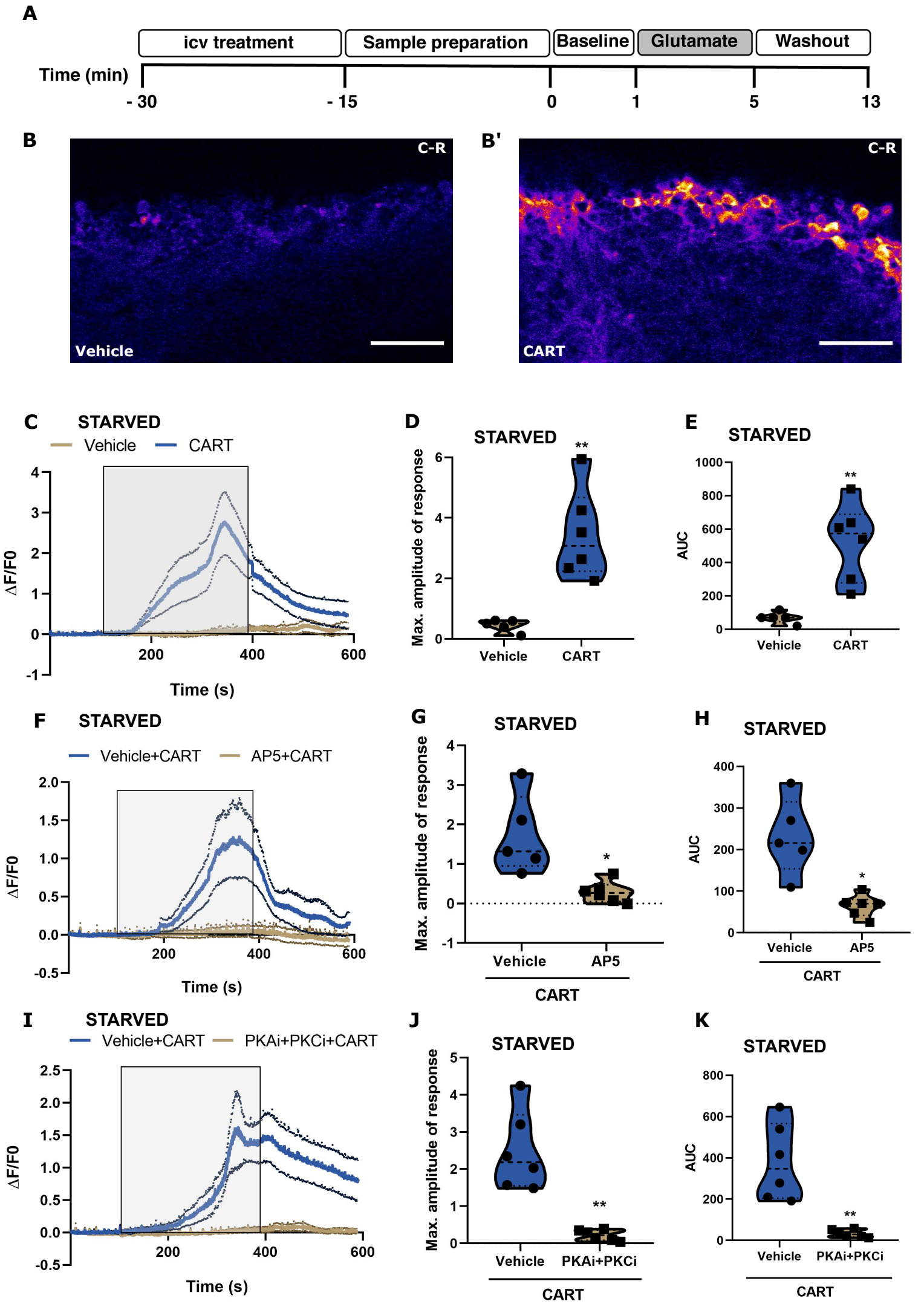
A
icv treatment
Sample preparation
Baseline
Glutamate
Washout
Time (min)
- 30
- 15
0
1
5
13
B
C-R
Vehicle
B'
C-R
CART
C
STARVED
Vehicle
CART
ΔF/F0
Time (s)
D
STARVED
Max. amplitude of response
Vehicle
CART
E
STARVED
AUC
Vehicle
CART
F
STARVED
Vehicle+CART
AP5+CART
ΔF/F0
Time (s)
G
STARVED
Max. amplitude of response
Vehicle
AP5
CART
H
STARVED
AUC
Vehicle
AP5
CART
I
STARVED
Vehicle+CART
PKAi+PKCi+CART
ΔF/F0
Time (s)
J
STARVED
Max. amplitude of response
Vehicle
PKAi+PKCi
CART
K
STARVED
AUC
Vehicle
PKAi+PKCi
CART

Figure 5

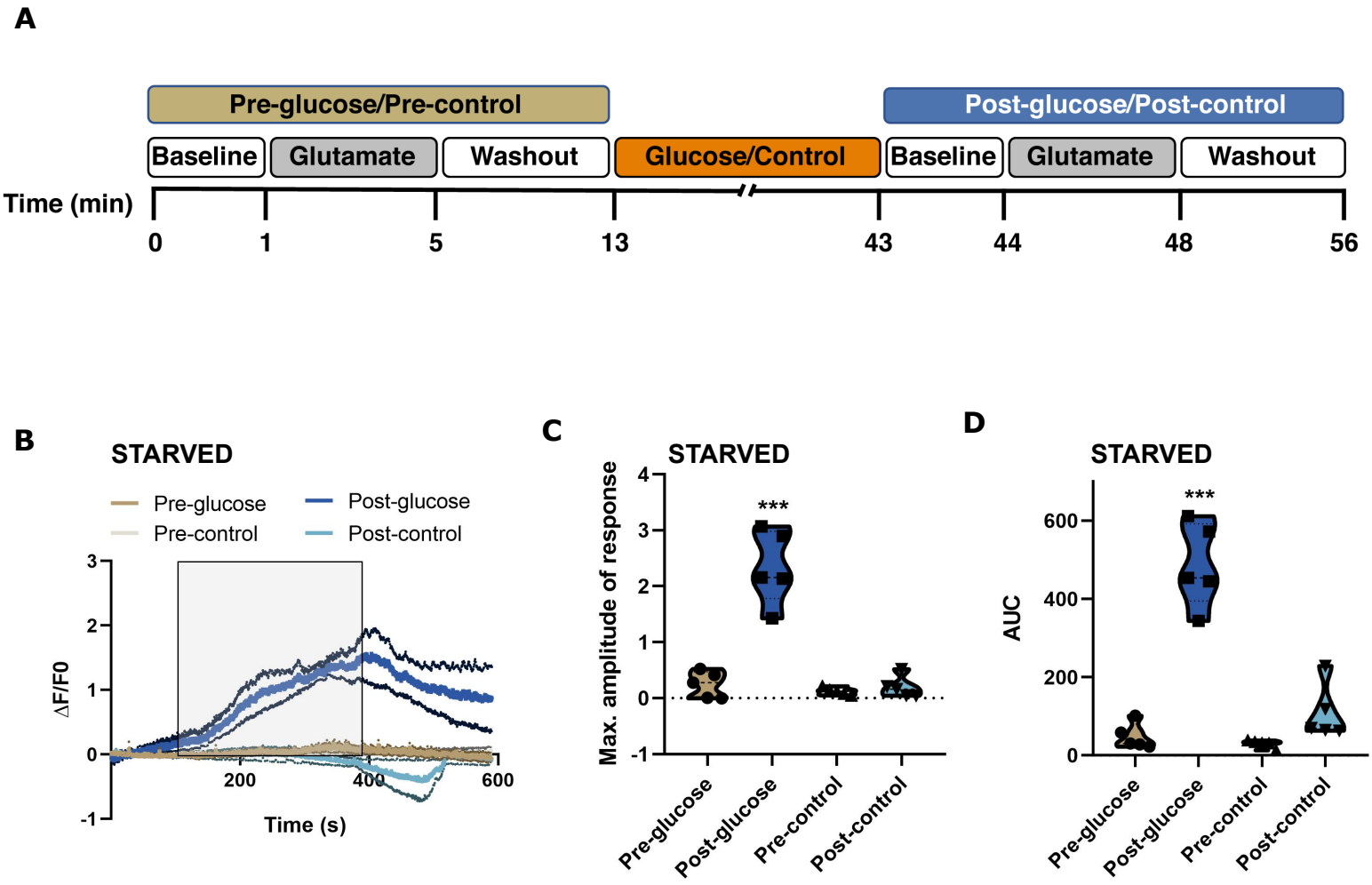
A
Pre-glucose/Pre-control
Post-glucose/Post-control
Baseline
Glutamate
Washout
Glucose/Control
Baseline
Glutamate
Washout
Time (min)
0
1
5
13
43
44
48
56
B
STARVED
Pre-glucose
Pre-control
Post-glucose
Post-control
ΔF/F0
Time (s)
C
STARVED
Max. amplitude of response
***
Pre-glucose
Post-glucose
Pre-control
Post-control
D
STARVED
AUC
***
Pre-glucose
Post-glucose
Pre-control
Post-control

Figure 6

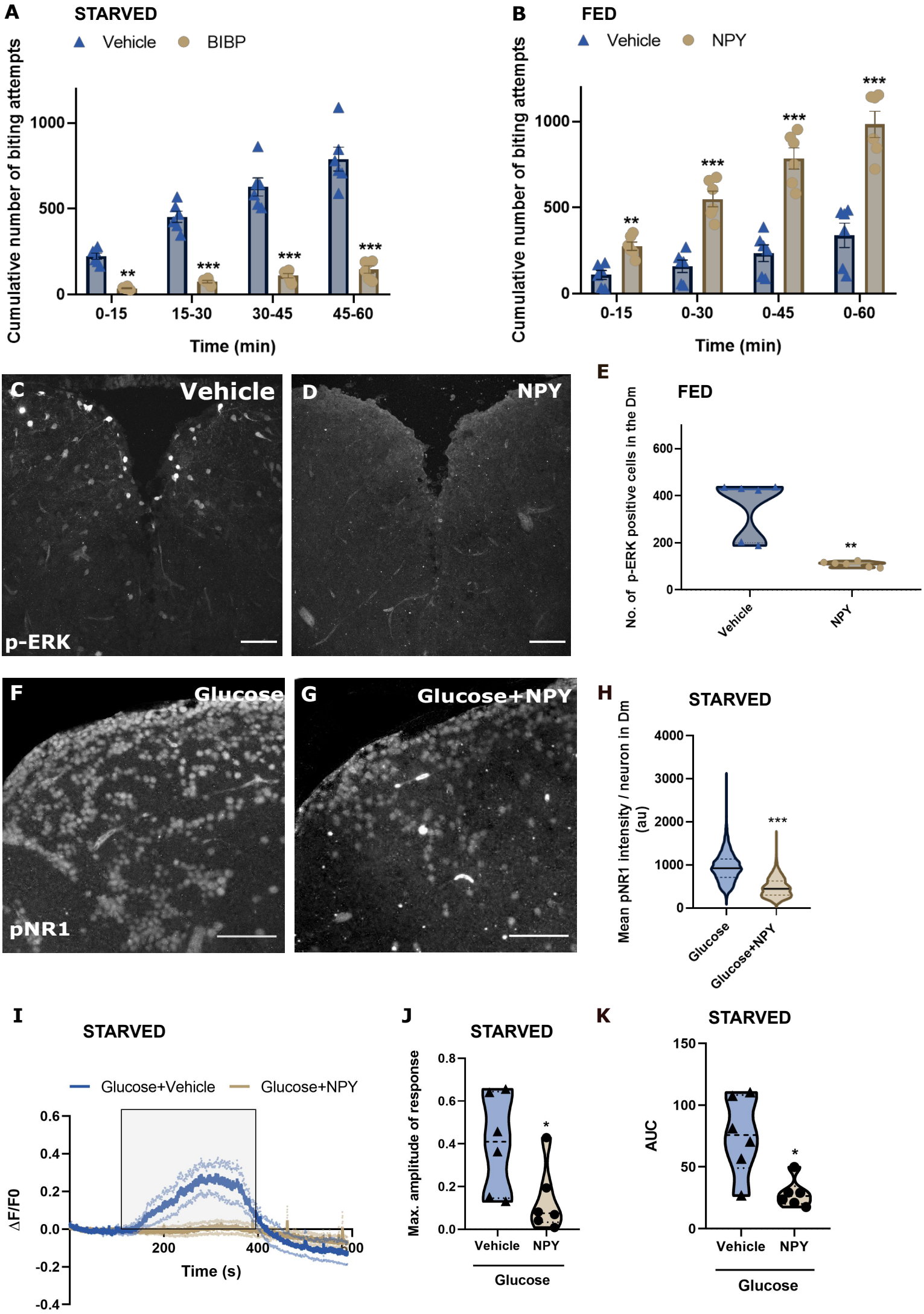
A
STARVED
Vehicle
BIBP
Cumulative number of biting attempts
1000
500
0
**
***
***
***
0-15
15-30
30-45
45-60
Time (min)
B
FED
Vehicle
NPY
Cumulative number of biting attempts
1000
500
0
**
***
***
***
0-15
0-30
0-45
0-60
Time (min)
C
Vehicle
p-ERK
D
NPY
E
FED
No. of p-ERK positive cells in the Dm
600
400
200
0
**
Vehicle
NPY
F
Glucose
pNR1
G
Glucose+NPY
H
STARVED
Mean pNR1 intensity / neuron in Dm (au)
4000
3000
2000
1000
0
***
Glucose
Glucose+NPY
I
STARVED
Glucose+Vehicle
Glucose+NPY
ΔF/F0
0.6
0.4
0.2
0.0
-0.2
-0.4
200
400
Time (s)
J
STARVED
Max. amplitude of response
0.8
0.6
0.4
0.2
0.0
*
Vehicle
NPY
Glucose
K
STARVED
AUC
150
100
50
0
*
Vehicle
NPY
Glucose

Figure 7

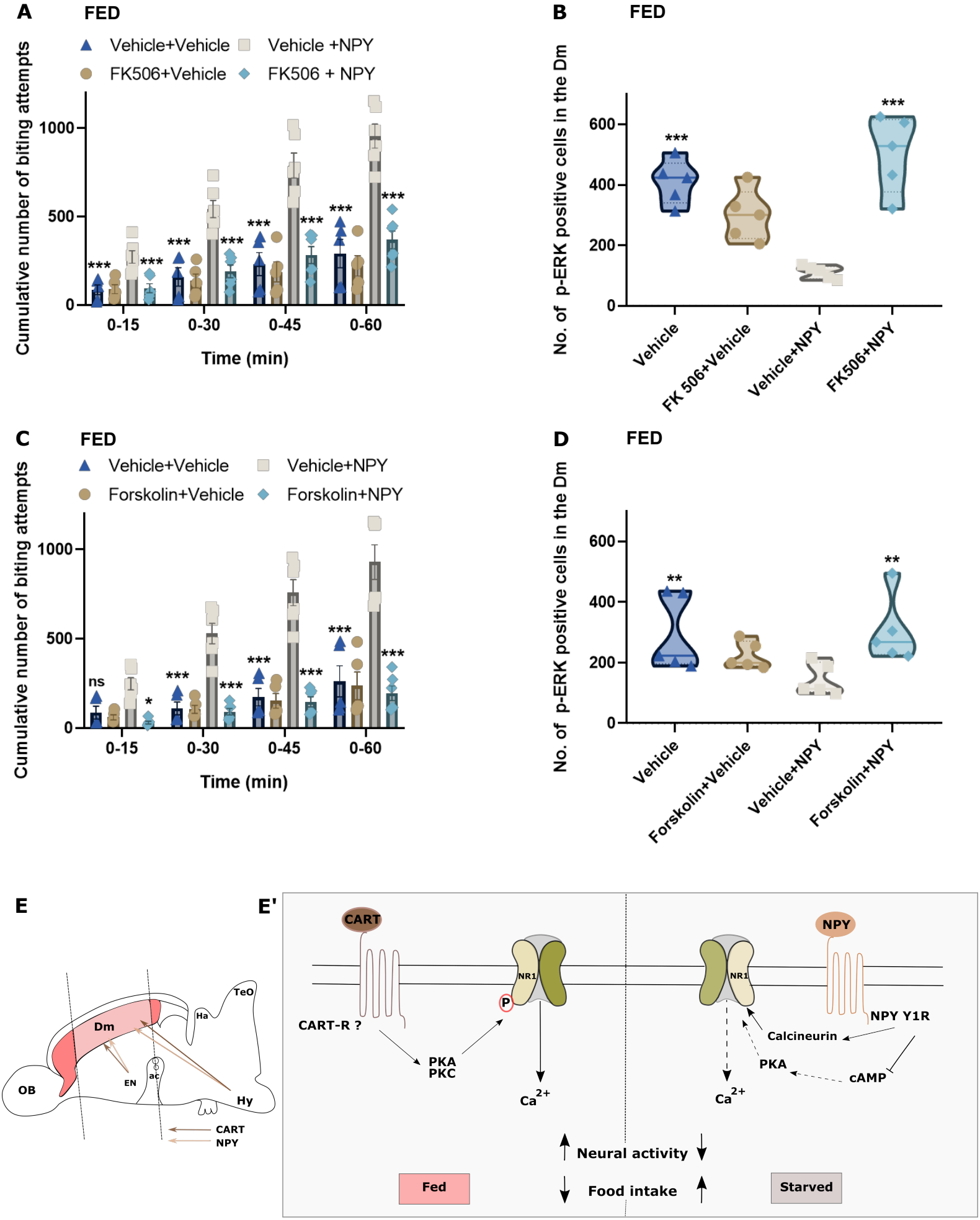
A
FED
Vehicle+Vehicle
Vehicle +NPY
FK506+Vehicle
FK506 + NPY
Cumulative number of biting attempts
1000
500
0
0-15
0-30
0-45
0-60
Time (min)
B
FED
No. of p-ERK positive cells in the Dm
600
400
200
0
Vehicle
FK 506+Vehicle
Vehicle+NPY
FK506+NPY
C
FED
Vehicle+Vehicle
Vehicle+NPY
Forskolin+Vehicle
Forskolin+NPY
Cumulative number of biting attempts
1000
500
0
ns
0-15
0-30
0-45
0-60
Time (min)
D
FED
No. of p-ERK positive cells in the Dm
600
400
200
0
Vehicle
Forskolin+Vehicle
Vehicle+NPY
Forskolin+NPY
E
TeO
Ha
Dm
OB
EN
ac
Hy
CART
NPY
E'
CART
NPY
NR1
P
CART-R ?
PKA
PKC
Ca2+
Calcineurin
PKA
cAMP
NPY Y1R
Neural activity
Food intake
Fed
Starved

Figure 8